Author:
Cadman, Ryan

Title:
The W102F mutation in the β3 auxiliary subunit of voltage-gated calcium channels prevents the augmentation of L-type calcium currents in tsA201 cells by the tau protein 4R0N-tau

UNIVERSITY OF BRISTOL

School of Physiology, Pharmacology and Neuroscience

MSc by Research

Start date: September 2021

Deadline: September 2023

The W102F mutation in the β_3 auxiliary subunit of voltage-gated calcium channels prevents the augmentation of L-type calcium currents in tsA201 cells by the tau protein 4R0N-tau

Word Count: 16,175

Author: Ryan Cadman
Student No: [redacted]
Email: wl18673@bristol.ac.uk

Supervisor: Professor Neil Marrion
Email: neilmarrion@gmail.com

A dissertation submitted to the University of Bristol in accordance with the requirements for the award of the degree of MSc by Research in the Faculty of Life Sciences. October 2023.

Acknowledgements

I am deeply grateful to my supervisor, Neil Marrion, for his incredible support and inspiration. I also want to extend my heartfelt thanks to Andrew Butler for teaching me so many exciting techniques and always being willing to help. This thesis would not have been possible without your guidance.

A big thank you to Emily Withers and Dany Bozadzhieva for creating a fun and supportive lab environment. I am also thankful to David Sheppard, who helped me get this thesis over the line. Lastly, I am thankful to my friends and family for their motivation and for making my time studying in Bristol truly wonderful.

List of Abbreviations

1,4-dihydropyridine: DHP

4-(2-hydroxythyl)-1-piperaineethanesulfonic acid: HEPES

Afterhyperpolarisations: AHPs

Alpha interaction domain: AID

Alzheimer's Disease: AD

Amino terminal interns (0, 1 or 2): 0N/1N/2N

Calcium-dependent inactivation: CDI

Calcium-induced calcium release: CICR

Calmodulin: CaM

Conserved interaction domain: CID

Dulbecco's modified eagle medium: DMEM

Ethylene glycol-bis(β-aminoethyl ether)-N,N,N',N'-tetraacetic acid: EGTA

Foetal bovine serum: FBS

Guanylate kinase domain: GK domain

High-voltage-activated: HVA

L-type calcium channel: LTCC

Long term Potentiation: LTP

Magnesium ATP: MgATP

Microtubule associated protein: MAP

Microtubule binding repeats (3 or 4): 3R/ 4R

Proline-rich domains: PRDs

SEM-5 SH3 domain at the C-terminus: SEM-5-CSH3

SEM-5 SH3 domain at the N-terminus: SEM-5-NSH3

SRC Homology 3 domain: SH3 domain

Tetraethylammonium chloride: TEACl

tsA201 cell line: transformed human kidney cell line

Voltage-gated calcium channels: VGCCs

Voltage-dependent inactivation: VDI

Abstract

L-type calcium channels (LTCCs) are voltage-gated calcium channels made up of three subunits, the α_1 pore-forming subunit and the β and $\alpha_2\delta$ auxiliary subunits. LTCC's have a wide range of cellular functions, including activation of the calcium-dependent components of the medium and slow afterhyperpolarisations (AHPs) in hippocampal neurons. AHPs are important for maintaining normal neuronal firing patterns. Tau is a microtubule associated protein (MAP) with six isoforms which have either three or four microtubule binding repeats (3R and 4R), and zero, one or two amino terminal inserts (0-2N). Preliminary evidence shows that the ratio of 3R:4R tau is imbalanced in Alzheimer's Disease (AD) and other dementias and causes an increase in number of LTCCs at the cell membrane of hippocampal neurons.

Previous research has shown that 4R0N-tau and 4R2N-tau, but not 4R1N-tau, augments L-type calcium currents in tsA201 cells, 4R0N-tau having the strongest effect. This interaction only occurs in LTCCs comprised of the α1C subunit ($Ca_v1.2$) and $Ca_v\beta3$ subunit isoforms and indicates that there is a direct interaction between 4R0N-tau and the $Ca_v\beta3$ subunit. The aim of this research is to determine the site of interaction within the $Ca_V\beta3$ subunit that mediates the proposed direct interaction between 4R0N-tau and $Ca_V\beta3$.

Electrophysiological experiments using tSA201 cell lines exogenously expressing $Ca_V1.2$, β3, and α2δ1 elicited L-type calcium current that was augmented when co-expressed with 4R0N-tau. Further electrophysiological experiments were conducted to find a point mutation which removed the augmentation of L-type calcium currents by 4R0N-tau. The W102F mutation of $Ca_v\beta3$ successfully achieved this aim without changing individual channel activity, assessed by calculating V0.5 and decay constant.

This research shows that mutation of a single tryptophan to phenylalanine, W102F, abolishes the ability of 4R0N-tau to augment L-type current. Increased concentrations of 4R0N-tau and upregulation of L type current has been reported in AD brains, and in aged animals experiencing cognitive decline, but not in aged animals that didn't experience cognitive decline. Therefore, the identification of the specific residue where the interaction between 4R0N-tau and $Ca_v\beta_3$ helps our understanding of AD pathomechanism and offers a potential therapeutic target for prevention.

Author's Declaration

I declare that the work in this dissertation was carried out in accordance with the requirements of the University's Regulations and Code of Practice for Research Degree Programmes and that is has not been submitted for any other academic award. Except where indicated by specific reference in the text, the work is the candidate's own work. Work done in collaboration with, or with the assistance of, others, is indicated as such. Any views expressed in the dissertation are those of the author.

SIGNED: Ryan Cadman

Date: 29/08/2024

Table of Contents

List of Figures

List of Tables

Chapter 1: General Introduction

1.1 Voltage-gated calcium channels (VGCCs)

VGCCs are a family of proteins that allow calcium ions to enter the cell when the membrane potential changes (Catterall, 2011). They are important for many cellular functions, such as muscle contraction, neurotransmitter release, and gene expression. VGCCs are classified into three main groups based on the structure and function of their α1 subunit, which forms the pore of the channel, Ca_v1-3 (Fox et al., 1987).

Ca_V1 are also called L-type channels, because they are activated by high or long-lasting depolarizations (Fox et al., 1987). They are sensitive to dihydropyridines, a class of drugs that can block or enhance their activity (Tikhonov and Zhorov, 2009). They are mainly found in cardiac, smooth, and skeletal muscle cells, where they mediate excitation-contraction coupling, as well as in neurons (Fox et al., 1987).

Ca_V2 are also called N-, P/Q-, and R-type channels, because they have different sensitivities to toxins from cone snails (ω-conotoxins) and spiders (ω-agatoxins) (Pei et al., 2000). They are activated by lower or shorter depolarizations than L-type channels (Cain and Snutch, 2011). They are mainly found in neurons and endocrine cells, where they mediate neurotransmitter and hormone release (Cain and Snutch, 2011).

Ca_V3 are also called T-type channels, because they are activated by low-threshold or transient depolarizations (Catterall et al., 2011). They are insensitive to dihydropyridines, ω-conotoxins, and ω-agatoxins (Bourinet and Zamponi, 2017). They are mainly found in neurons, cardiac pacemaker cells, and endocrine cells, where they modulate neuronal excitability, cardiac rhythm, and hormone secretion (Nanou et al., 2018).

1.2 Subunit composition of voltage-gated calcium channels

As shown in Figure 1, the α1 subunit forms the pore of VGCCs and allows the passage of Ca^{2+} through the channel. Many of the pharmacological and gating properties of LTCCs are governed by the identity of the α1 subunit (Lehmann-Horn and Jurkat-Rott, 1999). Due to the importance of the α1 subunit structure to normal function of LTCCs, its structural topology is highly conserved. It is made up of the cytoplasmic N- and C- terminal domains on each end (Figure 1B), between the N- and C- terminal domains are four transmembrane domains (I-IV) (Lehmann-Horn and Jurkat-Rott, 1999). Each of the transmembrane domains has six transmembrane α-helices (S1-S6), S1-S4 make up the voltage sensing domain, and S5-S6 the pore domain (Tuluc et al., 2016).

In addition to the α1 subunit, VGCCs have other subunits that modulate their activity and localization. These subunits are α2δ, β and γ (Dolphin, 2016).

As shown in Figure 1, The α2δ subunit is a complex of two subunits that are linked by a disulfide bond (Calderon-Rivera et al., 2012). The α2 subunit is extracellular and the δ subunit is transmembrane. Studies using heterologous expression systems, such as human embryonic kidney (HEK) cells, have demonstrated that co-expression of α2δ subunits with α1 and β subunits of VGCCs leads to increased calcium influx and altered channel properties (Qin et al., 2002). Additionally, imaging and biochemical techniques have shown that α2δ subunits are necessary for targeting VGCCs to specific cellular domains, such as lipid rafts (Robinson, 2011 ; Dolphin, 2016). Some drugs, such as gabapentin and pregabalin, bind to this subunit and inhibit VGCCs (Patel and Dickenson, 2016).

The β subunit is an intracellular subunit that interacts with the α1 subunit through its cytoplasmic domains (Buraei and Yang, 2010). In heterologous expression systems $Ca_v\beta$ regulates LTCC membrane trafficking and the resulting calcium currents (Buraei and Yang, 2013). In adult ventricular myocytes, disrupting the association between $Ca_v1.2$ and $Ca_v\beta$ affects the inactivation rate of LTCCs (Buraei and Yang, 2013). $Ca_v\beta$ also affects the expression and trafficking of the α1 subunit (Buraei and Yang, 2010).

The γ subunit is a transmembrane subunit that interacts with the α1 subunit through its extracellular domains. The function of the γ subunit is still being explored, but it is thought to have a role in modulating the voltage-dependence and kinetics of the channel, as well as affect the expression and trafficking of the α1 subunit (Kang and Campbell, 2003).

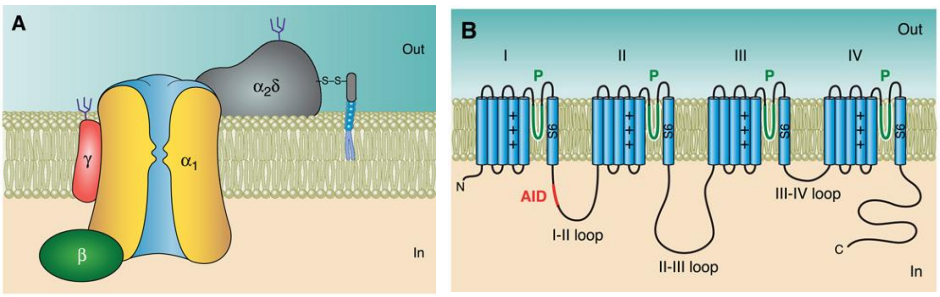

Figure 1 ***Diagrams showing structure of LTCC*** *A) Diagram showing subunit composition of LTCC B) Diagram showing transmembrane topology of the α1 subunit, AID - alpha interaction domain. Edited from Buraei and Yang, 2010*

1.3 L type calcium channels (LTCCs)

LTCCs are a family of high-voltage-activated (HVA) calcium channels that are sensitive to 1,4-dihydropyridine (DHP) drugs (Feng et al.,2018). They play important roles in various cellular processes, such as muscle contraction, hormone secretion, and gene expression (Feng et al., 2018). There are four isoforms of LTCCs, named $Ca_V1.1$, $Ca_V1.2$, $Ca_V1.3$, and $Ca_V1.4$, based on the structure and function of their α1 subunit, which forms the pore of the channel (Feng et al., 2018).

$Ca_V1.1$ is mainly expressed in skeletal muscle cells, where it mediates excitation-contraction coupling by triggering calcium release from the sarcoplasmic reticulum. It has a very slow activation and low calcium conductance compared to other LTCCs (Wu et al., 2016).

$Ca_V1.2$ is widely distributed in cardiac, smooth, and vascular muscle cells, as well as in neurons and endocrine cells (Bannister et al., 2013). It mediates excitation-contraction coupling in cardiac and smooth muscle cells, and regulates neurotransmitter and hormone release, gene expression, and neuronal excitability in other cell types. It has a fast activation and high calcium conductance compared to other LTCCs (Feng et al., 2018).

$Ca_V1.3$ is predominantly expressed in neurons and endocrine cells, especially in the brain, adrenal gland, and pancreas. It modulates neurotransmitter and hormone release, gene expression, and neuronal excitability by responding to low-threshold or transient depolarizations. It has a relatively low-voltage activation and fast inactivation compared to other LTCCs (Feng et al., 2018).

$Ca_V1.4$ is mainly expressed in the retina, where it mediates synaptic transmission between photoreceptors and bipolar cells. It has a low-voltage activation and slow inactivation compared to other LTCCs (Feng et al., 2018).

Cell afterhyperpolarizations (AHPs) are the phases of a neuron's action potential where the membrane potential becomes more negative than the resting potential (Matthews et al., 2009). They are also called the undershoot phases of the action potential. Cell afterhyperpolarizations can be classified into three types based on their duration and underlying mechanisms: fast, medium, and slow afterhyperpolarizations (fAHP, mAHP, and sAHP) (Matthews et al., 2009).

LTCCs are mainly involved in the generation of the mAHP and sAHP. The fast phase is carried by the calcium and voltage dependent BK channel and regulates firing at the onset of a burst lasting 25 ms, and is not reliant on calcium flow through LTCCs, as they are activated by N-type calcium channels (Marrion & Tavalin, 1998). The calcium dependent component of medium (50-100 ms) AHPs (Storm, 1987) is carried by SK channels which are selectively activated by LTCCs, making LTCCs essential for medium AHPs (Moyer et al., 1992; Lima and Marrion, 2007; Faber and Sah, 2007). Slow AHPs (1-2 s) are comprised of a calcium dependent component proposed to be mediated by SK1-IK heteromers (Higham et al., 2019).

LTCCs can also interact with ryanodine receptors, which are calcium-sensitive channels located on the endoplasmic reticulum. This interaction can trigger calcium-induced calcium release (CICR), which further enhances the calcium signal and activates more potassium channels for the sAHP (Sahu and Turner, 2021). The sAHP can also be influenced by other factors, such as sodium-potassium pumps, intracellular calcium buffers, and calcium extrusion mechanisms (Feng et al., 2018).

LTCCs open and close in response to changes in the membrane potential. They have four main states: closed, open, inactivated, and deactivated (Feng et al., 2018).

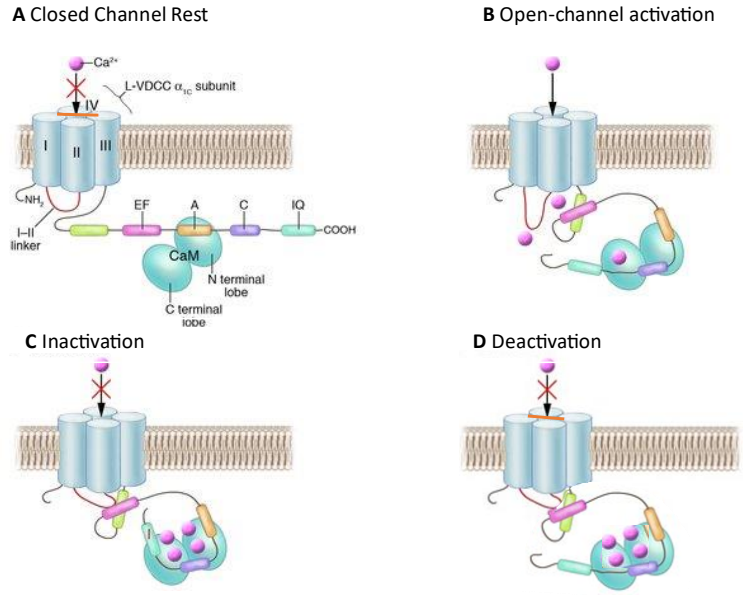

Figure 2 ***Gating of LTCCs*** *A) LTCC at rest when no calcium ion influx occurs. B) Upon depolarisation the LTCC undergoes conformational change, allowing calcium ion influx. C) After a time in the open state, the LTCC can become inactivated. D) when the membrane repolarises the LTCC can become deactivated. Edited from Bodi et al 2005.*

The channel is closed at the resting membrane potential, which is usually negative. The channel has a high affinity for calcium ions, but they cannot enter the pore because of a physical barrier formed by the S6 helices of the α1 subunit (Feng et al., 2018). The Calmodulin (CaM) is bound to peptide A, between the EF hand and IQ motif of the C terminus of the α subunit (Figure 2) (Bodi et al 2005).

When the membrane depolarizes, the voltage sensing S4 helices move outward, causing a conformational change in the channel that opens the activation gate. Calcium ions can now flow through the pore, which has a low affinity for them, and some calcium binds to CaM. In the open state, the EF hand prevents conformation of the inactivation gate (Figure 2). The channel stays open for a short time, depending on the magnitude and duration of the depolarization (Feng et al., 2018).

After being open for a while, the channel undergoes another conformational change that closes the inactivation gate. The calcium CaM complex undergoes a calcium dependent conformational change that relieves the pore blockage by the EF hand and allows the inactivation gate to close (Figure 2). This gate is formed by a loop between domains III and IV of the α1 subunit, which blocks the pore from the cytoplasmic side. The channel is still depolarized, but no longer conducts calcium ions. The channel can recover from inactivation by returning to the resting potential (Feng et al., 2018).

When the membrane repolarizes, the channel closes both the activation and inactivation gates, and returns to the closed state. However, the channel has a high affinity for calcium ions again, which can bind to the pore and stabilize it in a non-conducting state. This state is called deactivated, and it prevents the channel from reopening too quickly after repolarization. The channel recovers from deactivation when the calcium ions dissociate from the pore (Bodi et al., 2005; Feng et al., 2018).

These different states of L-type calcium channels allow them to regulate calcium entry into cells in a precise and dynamic manner, depending on the electrical and chemical signals they receive.

L-type calcium channels are selective for calcium ions because of the combined effects of electrostatic and steric forces in the channel pore. The pore is formed by four glutamate residues (EEEE locus) that coordinate the calcium ions and provide a high affinity binding site (Boda et al., 2009).

The electrostatic forces favour the entry of divalent cations (such as Ca^{2+}) over monovalent cations (such as Na^{+}) because they have a higher charge density and can interact more strongly with the negative charges of the glutamate residues (Boda et al., 2009).

Steric forces prevent the entry of larger cations (such as Ba^{2+} or Sr^{2+}) that have a similar charge density as Ca^{2+}, but a larger ionic radius. These cations cannot fit into the narrow pore and are excluded by repulsion from the channel's atoms (Boda et al., 2009).

Therefore, L-type calcium channels are selective for calcium ions because they can deliver the largest charge in the smallest ion volume, which minimizes the energy cost of dehydration and maximizes the electrostatic attraction with the channel pore.

The mechanism of L-type calcium channel inactivation involves two processes: voltage-dependent inactivation (VDI) and calcium-dependent inactivation (CDI). VDI is regulated by the $Ca_V\beta$ subunit, which interacts with the intracellular loop between domains I and II of the α1 subunit and causes a conformational change that closes the channel pore from the extracellular side. CDI is regulated by calmodulin (CaM), which binds to the C-terminal tail of the α1 subunit and causes a conformational change that closes the channel pore from the cytoplasmic side. Both processes are modulated by various factors, such as phosphorylation, redox state, and accessory proteins (Soldatov, 2012; Feng et al., 2018; Morales et al., 2019).

The importance of L-type calcium channel rate of inactivation for cell health lies in its role in controlling the duration and amplitude of calcium influx and the subsequent downstream effects on cellular functions. A proper balance between VDI and CDI is essential for maintaining the physiological calcium signalling and avoiding calcium overload or depletion, which can lead to various pathological conditions, such as arrhythmias, hypertrophy, apoptosis, and neurodegeneration (Morales et al., 2019; Feng et al., 2018; Soldatov, 2012; Tang and Rabkin, 2022; Kubalova, 2003).

1.4 Tauopathies

Tauopathies are a group of neurodegenerative diseases that are characterized by the abnormal accumulation and aggregation of a protein called tau in the brain (Guo et al., 2017). Tau is normally involved in stabilizing the microtubules that support the structure and function of neurons, but in

tauopathies, tau becomes hyperphosphorylated and detached from the microtubules, forming insoluble clumps called neurofibrillary tangles (Zhang et al., 2022b).

One of the intriguing features of tauopathies is that the tau pathology seems to spread from one brain region to another in a predictable pattern, following the anatomical connections between neurons. This suggests that tau aggregates can propagate from cell to cell, in a manner like prions, which are infectious proteins that cause diseases such as Creutzfeldt-Jakob disease (Kovacs et al., 2017; Takeda, 2019).

The mechanism of tau propagation is not fully understood, but it involves several steps: the release of tau aggregates from one neuron, either actively or passively; the uptake of tau aggregates by another neuron, through endocytosis or macropinocytosis; and the seeding of tau aggregation in the recipient neuron, by inducing the misfolding of normal tau (Takeda, 2019; Kovacs et al., 2017).

Tau propagation is thought to play a key role in the progression and severity of tauopathies, as well as in the diversity of clinical symptoms. Therefore, understanding and targeting tau propagation could be a promising strategy for diagnosing and treating these diseases (Takeda, 2019).

Tau protein has a natively unfolded structure, which means that it does not have a fixed three-dimensional shape, but rather adopts different conformations depending on its interactions with other molecules (Mandelkow et al., 2007). Tau protein can be modified by various post-translational modifications, such as phosphorylation, glycosylation, acetylation, and truncation, which can affect its function and aggregation (Avila et al., 2016).

Tau protein can also undergo alternative splicing, which is a process that generates different variants of the same protein from the same gene. In humans, there are six major tau isoforms that differ in the number of amino-terminal inserts (0N, 1N, or 2N) and microtubule-binding repeats (3R or 4R) in their structure (Iqbal et al., 2010). The 3R and 4R isoforms have different affinities and effects on microtubules, and their balance is important for maintaining normal neuronal function (Yasojima et al., 1999).

In healthy adult human brains, the 3R and 4R tau isoforms are expressed at a balanced ratio of about 1:1 (Yasojima et al., 1999). However, in some neurodegenerative diseases, such as AD, frontotemporal dementia, progressive supranuclear palsy, and corticobasal degeneration, this balance is disrupted by genetic mutations, environmental factors, or pathological processes. The imbalance of tau isoforms can

lead to abnormal tau aggregation, microtubule destabilization, axonal transport impairment, synaptic dysfunction, and neuronal death (Buchholz and Zempel, 2024). The ratio of 4R to 3R isoforms is increased in the hippocampus and midfrontal cortex of AD brains (Yasojima et al., 1999). Inducing this increased ratio in mice caused severe seizures and nesting behaviour abnormalities (Schoch et al., 2016) and overexpression of human 2N4R tau produced synaptic dysfunction and memory deficits in mice (Yin et al., 2016).

Commented [DS1]: Reference missing from reference list

It is thought that Tau protein tangles can interfere with the normal function and communication of brain cells, leading to their damage and death (Johnson and Jenkins 1999). The exact mechanism of how tau protein tangles cause cell death is not fully understood, but some possible factors include oxidative stress, inflammation, mitochondrial dysfunction, and impaired clearance of toxic proteins (Johnson and Jenkins 1999).

Recently the role of different tau isoforms in enhancing LTCC currents has been investigated in rat hippocampal neurons (Stan et al., 2022). Overexpression of the 4R0N-tau isoform enhanced LTCC-dependent components of medium and slow afterhyperpolarisations (Stan et al., 2022). Both 4R0N-tau and 4R2N-tau isoforms augment $Ca_v1.2$-mediated L-type currents when tsA-201 cells, but this effect was not observed with the 4R1N-tau isoform (Stan et al., 2022). The enhancement of calcium currents was linked to a physical association between tau and the $Ca_v\beta3$ subunit, which stabilised functional LTCCs in the membrane, increasing channel number and calcium influx (Stan et al., 2022). These findings suggest that the interaction between tau and calcium channels could contribute to cognitive impairments observed in early phases of tauopathies, such as AD (Stan et al., 2022). Following on from Stan et al., (2022), the interaction site within the 4R0N-tau isoform that mediates the augmentation of LTCC has been identified (Withers, 2023).

1.5 Hypothesis

A point mutation in the SH3 domain of $Ca_v\beta3$ will eliminate the effect of 4R0N-tau augmenting calcium currents of $Ca_v1.2$ LTCC

1.6 Aims

To determine the site of interaction within the $Ca_V\beta3$ subunit that mediates the proposed direct interaction between 4R0N-tau and $Ca_V\beta3$ (Stan et al., 2022). Finding this site will expand our knowledge on the mechanisms behind Tauopathies such as AD.

Chapter 2 Methods

2.01 Cell Maintenance

The tsA201 cell line (transformed human kidney cell line) was maintained in Dulbecco's Modified Eagle Medium (DMEM) (Gibco, MA, USA) supplemented with 10 % foetal bovine serum (FBS) (Gibco, MA, USA), penicillin and streptomycin (100 units/ml, Penicillin, 100 µl/mL, Streptomycin) (Gibco, USA, MA), known as DMEM+. The cells were kept in a 25 cm^2 cell culture flask, which was incubated at 37 °C and 5 % CO_2. To passage the cells, they were washed once in PBS, then incubated for 3-4 minutes at 37 °C in 2 ml PBS based calcium-free cell dissociation buffer. After the cells were dissociated and diluted in 6 ml DMEM+, the cells were then added to flasks in a 1:8 split (1 ml cell suspension to 7 ml DMEM+), 1:16 split (0.5 ml cell suspension to 7.5 ml DMEM+) or 1:32 split (0.25 ml cell suspension to 7.75 ml DMEM+). Cells seeded for transfection for patch-clamp recordings were added to 9.2 cm^2 tissue culture dishes (1-3 drops) as required, containing 1.5-2 ml DMEM+.

2.02 Preparation of Plasmids.

DH5α competent cells were used to introduce DNA into bacteria. The cells were thawed on ice and distributed into cold Eppendorf tubes. 5 µl of DNA were added to each tube and mixed gently. The tubes were then left to incubate on ice for 30 minutes. Next, the tubes were exposed to a brief 20 s heat shock and then incubated on ice for 2 minutes. 950 µl prewarmed super optimal broth media (a rich culture media) was then added to the tubes and incubated for 1 hour at 37 °C with mixing at 225 rpm. Then, 50 µl and 150 µl of the transformed cells were plated onto separate LB plates with 100 µg/ml ampicillin. The plates were then incubated overnight at 37 °C. The following day, single colonies were picked from the plates and grown in LB medium with ampicillin for 12-16 hours with mixing at 225 rpm. Mini, midi and maxi preps were prepared as needed using QuickLyse kits (Qiagen, Crawley, UK) according to the manufacturer's instructions.

2.03 Mutagenesis

There were two $Ca_v\beta3$ mutants used in these experiments, the first was the WW102,103AA (WW) mutation, the second was the W102F mutation, detailed in Table 1. DNA was sequenced by Eurofins using Sanger Sequencing, more detail about the mutant is discussed in Chapter 5.

WW Mutation: **Forward 5'** AGATTTTCTGCACATTAAAGAGAAGGCCAGCAATGACGCGGCGATCGGGAGGCTA **WT β3** GAGAAGTACAGCAATGACTGGTGGATCGGGAGGCTAGTGAAAGAAGGTGGCGATA **Reverse 3'** CTTCTTTCACTAGCCTCCCGATCGCCGCGTCATTGCTGGCCTTCTTTAATGTG Amino acid residues 102 & 103 substituted from Tryptophan to Alanine. TGG to GCG
W102F Mutation: **Forward 5'** CTTTCACTAGCCTCCCGATAAACCAGTCATTGCTGTACTT **WT β3** GAAAGAAGGTGGCGATATTGCCTTCATCCCCAGCCCCCAA **Reverse 3'** AAGTACAGCAATGACTGTTTATCGGGAGGCTAGTGAAAG Amino acid residue 103 swapped from Tryptophan to Phenylalanine TGG to TTT

Table 1 ***Sequences for the W102F and the WW mutations.***

Using the Stratagene QuickChange II XL kit, PCR mutations were performed following the manufacturer's instructions. Dpn I restriction enzyme was then added to the amplification reaction and centrifuged briefly. The mixture was incubated for 1 hour at 37 °C and transformed into ultracompetent cells with the Beta-mercaptoethanol mix from the kit. The mixture was then incubated on ice for 10 minutes and introduced the Dpn I-treated DNA into it. We followed the standard transformation procedure as described in Section 2.02 - Preparation of Plasmids.

2.04 Transfection

Cells were transfected using lipofectamine 2000 (Invitrogen, CA, USA) as per the manufacturer's instructions. Before transfection cells were left to recover from passaging for 24 hours in a 9.2 cm^2 tissue culture dish, incubated at 37 °C. After 24 hours the DNA was added into an Eppendorf with Optimem (Gibco, UK). Lipofectamine 2000 was also mixed with Optimem in a separate Eppendorf. These solutions were then left to incubate at room temperature for 5 minutes and then mixed and left to incubate at room temperature for 20 minutes. After the 20 minutes the DMEM+ the cells were growing in was replaced, and the transfection mixture was added to the cells and left overnight in an incubator set at 37°C. In the morning of the next day, cells were detached from the culture dish by incubation at 37°C with 2 ml PBS based enzyme free cell dissociation buffer for 4 minutes. Then, the plate was divided into 6 Petri dishes with 1-4 drops of cell solution in them, these plates were then returned to the 37 °C incubator to allow them to recover and adhere to the plates. The following day the Petri dishes were moved to a different incubator set at 27 °C to be used in experiments the following two days (explanation in Section 3.2.1). For these experiments 3 plasmids were required to express $Ca_v1.2$, and eGFP was required to identify transfected cells for patch-clamp experiments. 4 plasmids were used in each experimental condition to maintain consistency across the groups. 4R0N-tau and eGFP were co-expressed on a bisistronic vector. eGFP is a fluorescent protein that can be excited by light of wavelength 488-509 nm, as shown in Figure 4. The cells were visualised using a light microscope at 32x magnification. We mixed the DNA, lipofectamine 2000 and Optimem in fixed ratios as detailed in Table 2.

Group	DNA	Lipofectamine
Control	• 1 µg/15.3 cm^2 $Ca_v1.2$ (pIRES) • 1 µg/15.3 cm^2 $Cav\alpha_2\delta_1$ (pcDNA 3.1 +/hygro) • 1 µg/15.3 cm^2 $Ca_v\beta_3$ (pcDNA 3) • 1 µg/15 cm^2 eGFP (pEGFP-C3)	2.5 µl/1 µg of DNA
4R0N tau (WT & Mutant)	• 1 µg/15.3 cm^2 $Ca_v1.2$ (pIRES) • 1 µg/15.3 cm^2 $Ca_v\alpha_2\delta_1$ (pcDNA 3.1+/hygro) • 1 µg/15.3 cm^2 $Ca_v\beta_3$ (pcDNA 3) • 1 µg/15.3 cm^2 tau-eGFP (pIRES-eGFP)	2.5 µl/1 µg of DNA

Table 2 ***Amounts of plasmids*** *used in Transfection mixture.*

.

2.05 Solutions

Solutions used in electrophysiological experiments are detailed in Table 3. External and internal solutions were titrated to a pH of 7.4 using CsOH. These solutions enabled an electrode resistance of 2-5 MΩ.

Tetraethylammonium chloride (TEACl) was included in the external and internal solutions because it acts as a potassium channel blocker. By inhibiting voltage-gated potassium channels, TEACl ensured that there is no interference by potassium currents in the recordings.

4-(2-hydroxythyl)-1-piperaineethanesulfonic acid (HEPES) was used in the external and internal solutions to maintain a stable pH during experiments. This is crucial for ensuring that

the cellular environment remains consistent, which is important for accurate and reliable measurements. HEPES is highly soluble, membrane impermeable, chemically stable, and has minimal effects on biochemical reactions, making it an ideal buffering agent.

Calcium chloride ($CaCl_2$) was included in high concentration in the external solution to ensure that there was a sufficient concentration of calcium ions to generate measurable calcium currents (Fozzard, 2002; Liu, 2024).

Magnesium chloride ($MgCl_2$) was included in the external and internal solutions for several reasons. Magnesium ions block non-specific cation channels, which can otherwise interfere with the measurement of calcium currents. This ensured that the recorded currents were primarily due to calcium ions (Coulon, 2021). Magnesium ions can help stabilise the membrane potential by reducing the activity of other ion channels, particularly sodium and potassium channels (Coulon, 2021). High concentrations of calcium ions can lead to cellular toxicity and affect the accuracy of the measurements. Magnesium ions help to modulate the influx of calcium ions, preventing calcium overload and maintaining cellular health during the experiment (Coulon, 2021).

D-Glucose was included in the external solution for several important reasons. D-Glucose serves as a primary energy source for cells, ensuring that they remain metabolically active and healthy during experiments (Yuan and Atchison, 2019). It helps maintain normal cellular functions, including ion transport and membrane potential, which are crucial for accurate electrophysiological measurements (Yuan and Atchison, 2019). Including D-Glucose in the solution helps to replicate the natural extracellular environment, providing conditions like those found in vivo (Yuan and Atchison, 2019). D-glucose is also used to adjust the osmolarity of the external solution to prevent cell swelling during whole-cell recording and the activation of stretch-activated ion channels.

Cesium methanesulfonate ($CsMeSO_3$) is commonly used in internal solutions for electrophysiology, particularly in patch-clamp techniques, for several reasons. Cesium ions act as effective blockers of potassium channels. This is crucial to ensuring there is no interference from potassium currents in the experiments. Methanesulfonate is not transported through chloride channels, making it a suitable anion for internal solutions. This

helps in maintaining the desired ionic environment inside the cell, which is essential for accurate and reproducible measurements in electrophysiological studies.

Magnesium ATP (MgATP) was used in the internal solution for several important reasons. ATP is a primary energy source for many cellular processes, including the activity of ion pumps and transporters. MgATP provides the necessary energy to maintain the proper function of these proteins during recordings. Magnesium ions help stabilise the structure of ion channels and other proteins, ensuring their proper function, this is crucial for accurate measurements (Cui et al., 2021). ATP is involved in involved in phosphorylation reactions, which are essential for the regulation of many ion channels and transporters. These reactions can modulate the activity of these proteins, affecting the overall ionic currents measured during experiments (Cheng et al., 1991).

Ethylene glycol-bis(β-aminoethyl ether)-N,N,N',N'-tetraacetic acid (EGTA) was used in the internal solution for several key reasons. EGTA is a calcium chelator, meaning it binds to calcium ions and helps control their concentration within the cell. This is crucial for experiments where precise regulation of intracellular calcium levels is necessary. EGTA has a high affinity for calcium ions, allowing it to effectively buffer and stabilise the intracellular calcium concentration. This helps in maintaining a consistent experimental environment (Manz et al., 2021). By chelating calcium, EGTA can minimise calcium-dependent processes that might interfere with the measurements being taken.

Ext ernal		Internal	
Chemical	Concentration (mM)	Chemical	Concentration (mM)
TEACl	140	$CsMeSO_3$	120
HEPES (acid)	10	TEACl	20
$CaCl_2$	5	$MgCl_2$	1
$MgCl_2$	1	MgATP	4
D-GLUCOSE	10	HEPES (Na)	10
		EGTA	5

Table 3 ***The components of the external and internal solutions used in electrophysiological experiments.***

2.06 Electrodes and recording set up.

3"", 1.5 mm OD 0.86 mm ID filamented capillaries (World Precision Instrument, Shanghai, China) were fabricated using a Narishige Puller (model PP-830) and fire polished using a

Narishige micro forge (model MF-830) to aid sealing. The electrode was then inserted into an electrode holder with a silver wire coated with a layer of Ag/AgCl. This coating was achieved using electrolysis with a 0.9 % NaCl saline solution – the wire acting as a positive electrode, attracting the Cl ions onto its surface. The wire was recoated weekly for the duration of the project.

The wire and electrode were inserted into an electrode holder, which was placed onto a CV201A Headstage (Molecular Devices, CA, USA) which was connected to a PatchStar Micromanipulator (Scientifica, UK). An inverted microscope was used with an ultraviolet light source (Zeiss Axiovert 100, Germany) with an experimental platform to mount cell culture dishes. All this equipment was mounted on an anti-vibration table contained within a Faraday cage which prevents vibrations and electromagnetic interference from the surroundings interfering with recordings.

Before recording, cell culture dishes were mounted in the experimental platform with external solution constantly circulating at a rate of 2-8 ml/min using a Watson Marlow 505S peristaltic pump. The solution was initially drained into a waste bucket until the DMEM+ solution which the cells were incubated in was drained from the cell culture dish and replaced with external solution, at which point the end of the outflow tube was removed from the waste bucket and placed in a well of external solution to form a circuit. This was done as the presence of the DMEM+ solution would prevent formation of seals between cells and patch pipettes.

2.07 Software

Patchmaster (HEKA, Germany) was used to carry out voltage protocols. The currents from which were recorded using an Axopatch 200A patch-clamp amplifier (Molecular Devices, CA, USA). Ionic currents were low-pass filtered at 1 kHz using an 8-pole Bessel filter (Frequency Devices, IL, USA) and acquired at a sampling rate of 10 kHz using Pulse.

2.08 Electrophysiology

Whole-cell voltage-clamp recordings were made from visually identified tsA201 cells expressing eGFP (Figure 4). Series resistance and pipette capacitance were 95 % compensated. During the current measurements, the cells were held at -80 mV then the voltage was stepped from -50 mV to 70 mV in 10 mV increments. Evoked currents were leak subtracted using a P/4 protocol. The Axon Digidata 1550B Data Acquisition System (Molecular

Devices, CA, USA) was used to convert analogue to digital data signals and vice versa. All experiments were conducted at room temperature. All currents were normalised to cell capacitance for data analysis, the value of capacitance for a cell was approximately 17.5 pF.

2.09 Data Analysis

Patchmaster was used to measure the peak current amplitude at each voltage step and generate IV curves. The membrane potential was plotted against current using Prism 9 which was also used to perform a two-way ANOVA with multiple comparisons to test the statistical significance between current voltage relationships. A two-way ANOVA was chosen because there were two variables (voltage and Cavβ) with more than two variables for any one of them. The conductance was calculated from the peak current amplitude (+20 mV) (assuming a reversal potential of +70 mV, based on IV curve extrapolation) using the formula $G = I/(V - Vrev)$. The conductance was normalised (G/Gmax) and plotted against voltage. The curves were fitted with the Boltzmann distribution and the V0.5 and slope calculated in Prism 9. Unpaired t-tests were used for comparing V0.5 and slope between 2 groups, and one-way ANOVA for comparing 3 groups. A single exponential was fitted to the current decay generated by steps to 0, +10, +20 and +30 mV, which gave the best resolution of the inward current. A single exponential was used because a double exponential was inconsistent between cells, probably due to the short pulse length that did not allow for a clear resolution of the slower exponential. The current decay was plotted against voltage in Prism 9 and a two-way ANOVA used to test the statistical significance between groups with or without 4R0N-tau expression, in both WT and mutant conditions.

Chapter 3: Characterisation of currents

3.1 Introduction

The voltage-dependent activation of L-type calcium channels differs between subtypes, depending on their biophysical properties and expression patterns. The four subtypes of L-type calcium channels are $Ca_v1.1$, $Ca_v1.2$, $Ca_v1.3$, and $Ca_v1.4$. They have different voltage thresholds, activation kinetics, and inactivation rates. For example, $Ca_v1.1$ and $Ca_v1.2$ have higher activation thresholds (around -40 mV) and faster activation kinetics than $Ca_v1.3$ and $Ca_v1.4$, which have lower activation thresholds (around -60 mV) and slower activation kinetics (Lipscombe at al., 2004).

The β subunit of L-type calcium channels has a significant impact on the voltage-dependent activation of the channel. The β subunit interacts with the intracellular loop between domains I and II of the α1 subunit and modulates its voltage sensitivity and gating kinetics. The β subunit can shift the voltage dependence of activation to more negative potentials, increase the open probability of the channel, and accelerate the activation and deactivation kinetics. The β subunit can also affect the coupling between voltage sensing and pore opening, as well as the cooperativity between subunits within a channel complex. Different isoforms of the β subunit (β1-β4) can have different effects on the channel function, depending on their expression levels and binding affinities (Hullin et al., 2003).

The subtypes of L-type calcium channels are separated by pharmacology based on their different sensitivities and affinities to various drugs that act as agonists, antagonists, and blockers of channel function. Agonists bind to the channel and increase its open probability, allowing more calcium influx. Examples of agonists are FPL64176 and (S)-(-)-BayK8644, which have pEC 50 values of ~7.8 for L-type calcium channels (Thomas et al., 1985; Fan et al., 2001).

Antagonists and blockers bind to the channel and decrease its open probability, reducing calcium influx. Examples of antagonists are nilvadipine and nimodipine, which are dihydropyridines that have pIC 50 values of 6.3 and ~6.0, respectively, for L-type calcium channels (Rosenthal, 1994; Carlson et al., 2020). Examples of blockers are verapamil and diltiazem, which are phenylalkylamines that have pIC 50 values of ~5.0 and 4.2, respectively, for L-type calcium channels (Chen et al., 2013).

The subtypes of L-type calcium channels have different affinities for these drugs, depending on their structural and functional properties. For example, $Ca_v1.1$ and $Ca_v1.2$ have higher affinity for dihydropyridines than $Ca_v1.3$ and $Ca_v1.4$, while $Ca_v1.3$ and $Ca_v1.4$ have higher

affinity for phenylalkylamines than $Ca_v1.1$ and $Ca_v1.2$. Therefore, pharmacology can be used to distinguish between the subtypes of L-type calcium channels and modulate their activity in different tissues and cells. Nimodipine is a dihydropyridine calcium channel blocker that binds to the α1 subunit of the L-type calcium channel, which forms the pore and the voltage sensor of the channel.

Nimodipine binds preferentially to the inactive state of the channel, which is stabilized by membrane hyperpolarization or repolarization. By binding to the inactive state, nimodipine prevents the channel from returning to the closed state, which is necessary for subsequent activation by depolarization (Striessnig et al., 2014).

Nimodipine also binds to the open state of the channel, but with lower affinity than to the inactive state. By binding to the open state, nimodipine blocks the channel pore and inhibits calcium influx. Therefore, nimodipine inhibits L-type calcium channels by two mechanisms: state-dependent inhibition and pore blockade. Both mechanisms reduce the availability and conductance of the channel, leading to decreased calcium entry and vascular smooth muscle relaxation (Striessnig et al., 2015).

The effect of nimodipine on L-type calcium channels is dependent on the holding potential, which is the membrane potential before a depolarizing stimulus. The holding potential determines the proportion of channels that are in the closed, open, or inactive states (Streissnig et al., 2015).

At more negative holding potentials (e.g., -80 mV), most channels are in the closed state, which has low affinity for nimodipine. Therefore, nimodipine has little effect on these channels until they are activated by depolarization. At more positive holding potentials (e.g., -40 mV), some channels are in the open state, which has moderate affinity for nimodipine. Therefore, nimodipine can block these channels and reduce calcium influx. However, some channels are also in the inactive state, which has high affinity for nimodipine. Therefore, nimodipine can also prevent these channels from recovering and being activated again. At intermediate holding potentials (e.g., -60 mV), most channels are in a dynamic equilibrium between the closed and open states, with a small fraction in the inactive state. Therefore, nimodipine can affect both the activation and inactivation kinetics of these channels, depending on the frequency and duration of depolarization (Streissnig et al., 2015).

In summary, nimodipine antagonizes L-type calcium channels by binding to different states of the channel with different affinities. The effect of nimodipine is dependent on the holding

potential, which determines the distribution of channel states and their responsiveness to depolarization.

3.2 Results

3.2.1 Optimisation of Protocol

The protocol previously being used in the lab had exceptionally low successful expression and current size (Figure 3). To improve the protocol, low temperature rescue was used to improve expression and current size (Denning et al., 1992; Sheppard, 2011; Wang et al., 2018). Low temperature rescue involves incubating cells overnight at 27 °C instead of 37 °C, which increases expression of larger proteins. Table 4 shows the changes made to the protocol.

	Day 1	**Day 2**	**Day 3**	**Day 4**	**Day 5**
Old Protocol	Transfect cells and move into 37°C	Split cells, return to 37 °C	Perform electrophysiological studies	Perform electrophysiological studies	Perform electrophysiological studies
New Protocol	Transfect cells and move into 37°C	Split cells, return to 37 °C	Move cells into 27°C	Perform electrophysiological studies	Perform electrophysiological studies

Table 4 ***Comparison of Old Protocol and New Protocol*** *shows changes made from previous protocol, utilising low temperature rescue.*

The new protocol was successful in increasing both expression (elicited measurable current) and current size (Figure 3). These marked differences are likely to be due to improved trafficking of the L-type Ca channels to the plasma membrane or the decreased trafficking of the L-type Ca channels away from the plasma membrane due to the lower temperature.

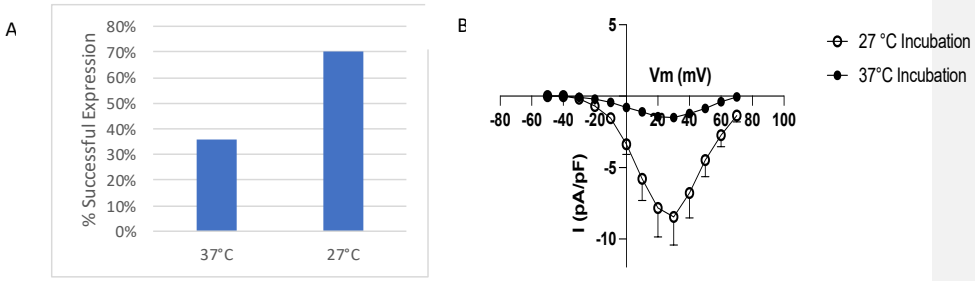

Figure 3 **The new protocol improves both successful expression and current size** *A) Bar chart showing marked increase in successful expression using low temperature rescue (37 °C N=83, 27 °C N=85).* B) *24-hour incubation in 27 °C causes a marked increase in calcium current (27 °C N=6, 37 °C N=6)* Reproduced with permission of Emily Withers.

3.2.2 Transfected tSA-201 cells have no endogenous Calcium current.

To establish whether tSA-201 cells showed endogenous calcium current that would interfere with the results, untransfected cells were studied using a patch-clamp protocol using a protocol which stepped the voltage from -80 mV to +70 mV in 10 mV increments. These results were compared with cells expressing exogenous Cav1.2, β3, α2δ1 (and eGFP). As shown in Figure 4, untransfected tSA-201 cells elicited no endogenous calcium current, whereas Cav1.2-transfected cells expressed currents characteristic of LTCC, therefore tSA-201 cells are an appropriate model for investigating calcium currents. Cells that were successfully transfected were identified by the fluorescence of eGFP, approximately 70 % of cells expressing eGFP displayed a net inward current.

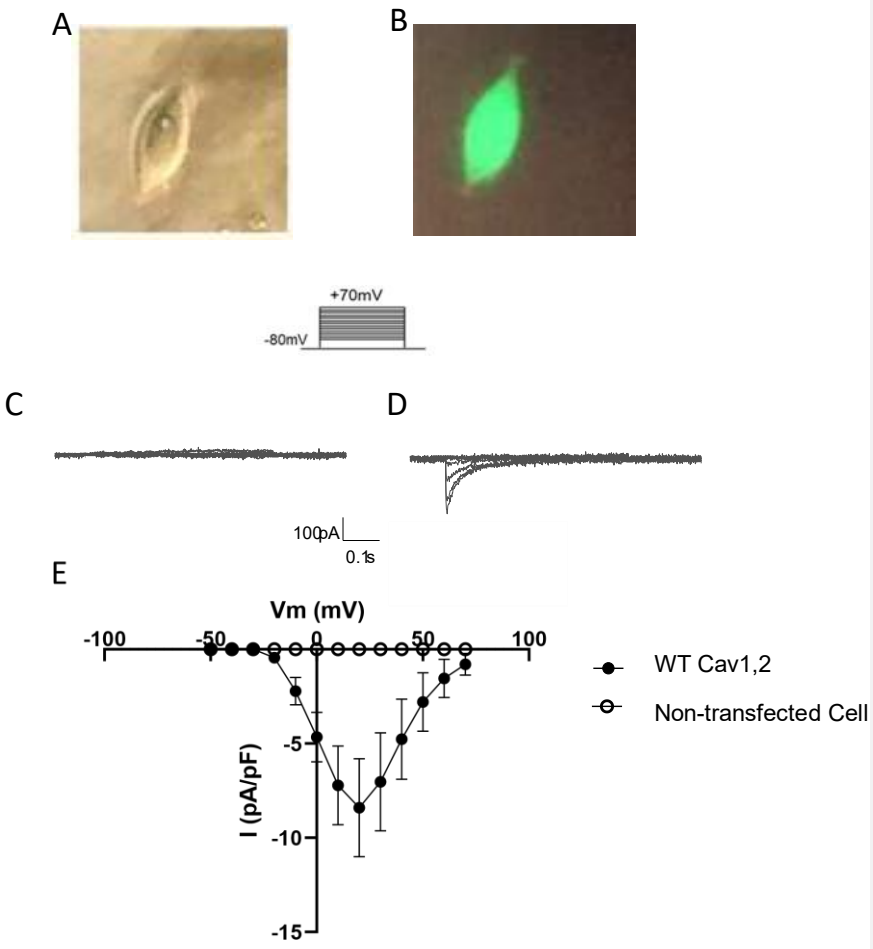

Figure 4 ***tsA-201 cells have no endogenous calcium current****. A) shows a phase contrast image of a cell and B) shows eGFP fluorescence from the same cell. C) shows the traces of a non-transfected cell undergoing the voltage protocol used to acquire whole-cell currents shown above. D) shows the traces from a cell exogenously expressing Cav1.2. E) shows is showing an IV curve comparing non-transfected cells and cells expressing* $Ca_v1.2$ *(Images in A and B reproduced by permission of Emily Withers)*

3.2.3 Characterisation of Current

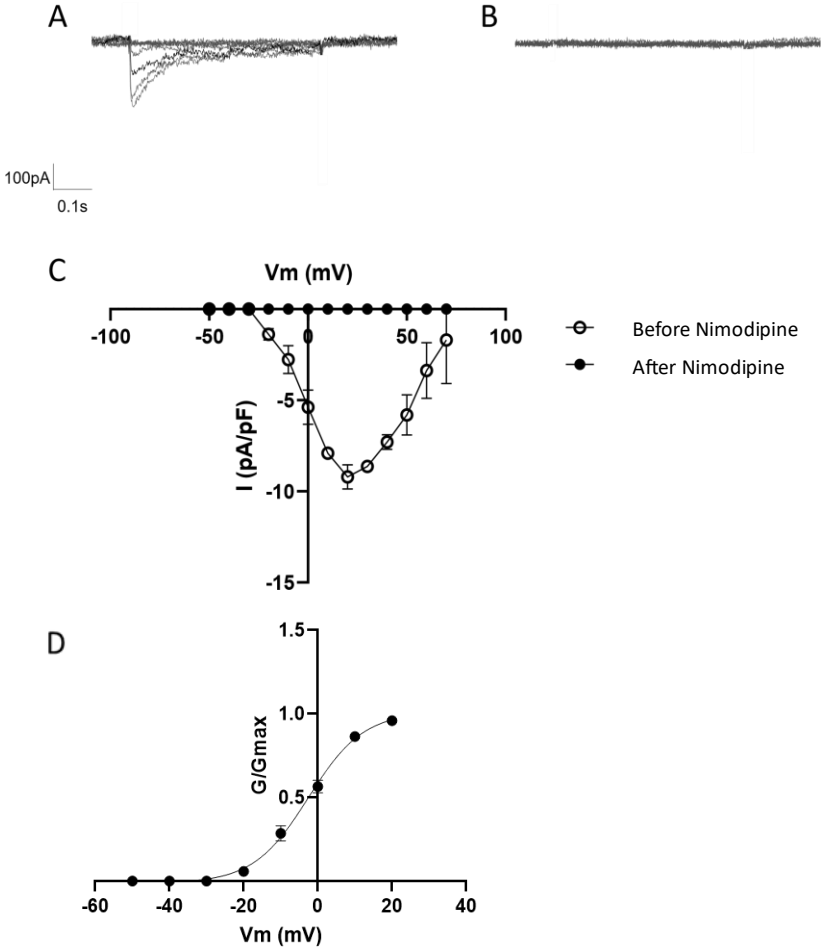

Figure 5 **Nimodipine *blocks calcium current in tSA-201 cells exogenously expressing LTCCs*.** *A) Representative traces from a cell undergoing voltage steps from -50mV to 70mV in 10mV increments. B) Representative traces from the same cell with 10μM Nimodipine present. C) IV plot comparing the traces* (n=22) *D) shows an activation curve for currents elicited in the absence of nimodipine.*

The experiments in this chapter were performed to characterise the observed currents. Figure 5 shows analysis of currents elicited from tsa-201 cells expressing $Ca_v1.2$, $Ca_V\alpha2\delta1$, β_3. The average V0.5 value calculated from the activation curve (Figure 5D) was -2.5 ± 1.4 mV.

Nimodipine was used to demonstrate that the pharmacology of the expressed $Ca_v1.2$, $Ca_V\alpha2\delta1$, β_3 agrees with literature, as it is a selective LTCC inhibitor (Carlson et al., 2020). Once a control current had been generated (absence of nimodipine) using standard solutions, the external solution was swapped to one containing 10 µM nimodipine. The cell then underwent the same protocol until the decrease in current had stabilised. An IV was plotted comparing the two conditions using the peak currents elicited at each voltage step (Figure 5C).

In the absence of nimodipine, peak LTCC were approximately 10 pA/pF, when nimodipine was added there was no current. This shows that nimodipine blocks any calcium current flow through the exogenously expressed LTCC.

3.3 Discussion

This chapter shows that tsA201 cells are an appropriate model for investigating LTCCs and the characterisation of the Ca^{2+} currents elicited from tSA-201 cells expressing $Ca_v1.2$, $\alpha2\delta1$ and β_3. Figure 5 shows that the voltage dependence of activation of the channels matches the literature, V0.5 = -2.5 ± 1.4 mV, compared to V0.5 = -2.4 ± 1.0 mV (Stan et al., 2022). These figures can only be compared with experiments using the same subunit combination, as when different isoforms are expressed, the activation curve is shifted (Stan et al., 2022).

Figure 5 shows that the currents being measured are L-type currents. Nimodipine is a selective LTCC antagonist, so will only block L-type currents (Carlson et al., 2020), this can be seen in Figure 5 as presence of nimodipine stops any current being elicited from cells which previously elicited current. A high concentration (10 µM) of nimodipine was used to ensure the full effect was seen. The antagonistic effect of nimodipine on calcium channels is dependent on holding potential (Streissnig et al., 2015). At a holding potential of -80 mV (the same as was used in the experiments), the IC50 of nimodipine was found to be 2000 nM, whereas at a holding of -30 mV the IC50 was found to be 52 nM (Streissnig et al., 2015). Nimodipine acts by binding to the $Ca_v1.2$ subunit of LTCCs and acting as a negative allosteric modulator, the binding of nimodipine causes the structure of the LTCC to change, disrupting the calcium ion binding sites (Zink et al., 2020).

Chapter 4: Presence of 4R0N-tau augments calcium current through LTCCs

4.1 Introduction

Several studies have implicated calcium upregulation in brain aging and AD (Thibault et al., 1998; Thibault et al., 2007). One possible explanation for calcium upregulation in brain aging is that the voltage gated LTCCs, which mediate calcium influx into neurons, become more sensitive and active in aged neurons, leading to increased intracellular calcium levels (Moore and Murphy, 2020). This may result from changes in the expression, phosphorylation, or redox state of the channel subunits or their modulators (Moore and Murphy, 2020).

Calcium upregulation in brain aging can affect the medium and slow afterhyperpolarizations (mAHP and sAHP), which are calcium-dependent potassium currents that follow a burst of action potentials and limit further neuronal firing. The mAHP is mediated by SK channels, while the sAHP is mediated by SK1-IK heteromers (Xia et al., 1998; Dwivedi and Bhalla 2021). Both mAHP and sAHP are increased in hippocampal neurons from aged animals, and this correlates with impaired learning and memory (Matthews et al., 2009). The enhanced mAHP and sAHP may reflect the increased calcium influx via L-type calcium channels, as well as altered calcium buffering and release from intracellular stores.

Nimodipine is a drug that blocks L-type calcium channels and reduces calcium influx into neurons. Nimodipine has been shown to decrease the amplitude of the sAHP in aged neurons, but not in young neurons (Power et al., 2002). This suggests that the sAHP in aged neurons is more dependent on L-type calcium channels than in young neurons. Nimodipine also enhances cognition in aged animals and humans, as measured by various tasks that involve hippocampal function, such as eyeblink conditioning and spatial memory (Disterhoft et al., 1996). This suggests that nimodipine improves neuronal excitability and synaptic plasticity by reducing calcium overload and sAHP in aged neurons.

It has been shown that overexpression of two tau isoforms, 4R0N and 4R2N, in rat hippocampal neurons or in tsA-201 cells (a cell line derived from human embryonic kidney cells) increased the L-type calcium current and the calcium-dependent afterhyperpolarizations (AHPs), which are potassium currents that limit neuronal firing. However, this effect was not observed with another tau isoform, 4R1N, or with other types of calcium channels (Stan et al., 2022).

The enhancement of L-type calcium current by 4R0N and 4R2N tau was dependent on the presence of a specific β subunit, Ca_Vβ3. When the α1 subunit (Ca_V1.2) was co-expressed with Ca_Vβ3, both 4R0N and 4R2N tau increased the current amplitude and the number of functional channels in the membrane, as measured by non-stationary noise analysis. However, when the α1 subunit was co-expressed with another β subunit, Ca_Vβ2a, neither 4R0N nor 4R2N tau had any effect on the current or the channel number (Stan et al., 2022).

The mechanism underlying this isoform-specific and subunit-dependent modulation of L-type calcium current by tau involves a direct physical interaction between tau and Ca_Vβ3. Co-immunoprecipitation experiments showed that 4R0N tau and Ca_Vβ3 were associated in a complex, while 4R1N tau and CaVβ3 were not (Stan et al., 2022). Moreover, mutagenesis studies identified a region in the N-terminal repeat of 4R0N-tau that was essential for binding to Ca_Vβ3 and for augmenting L-type calcium current (Withers, 2023).

4.2 Results

To investigate how 4R0N-tau increases LTCCs, two groups of transfected tsA201 cells were used to investigate the effect of 4R0N-tau on Ca_v1.2 mediated inward current. The control group expressed Ca_v1.2, α2δ1, β_3 and eGFP, the experimental group expressed the same subunits but eGFP was replaced with a vector containing 4R0N-tau and eGFP.

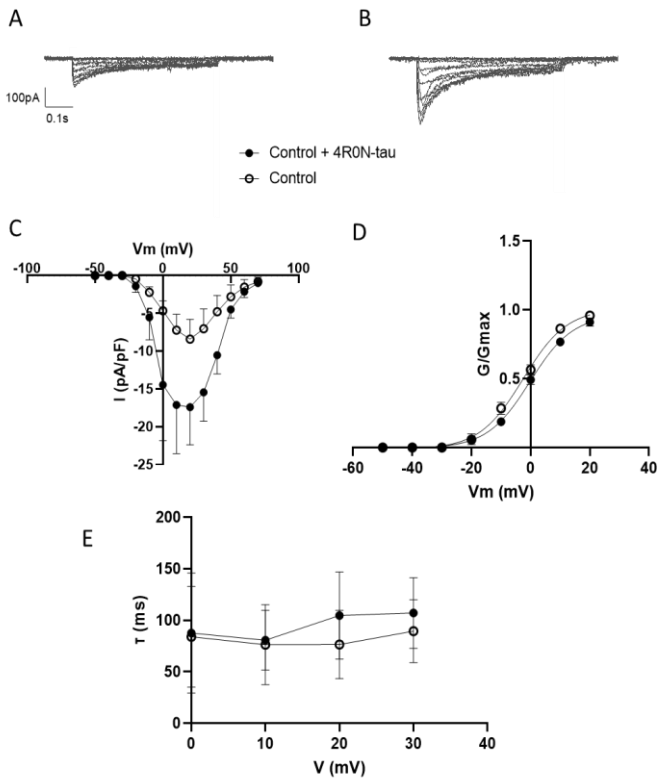

Figure 6 ***There is significant difference between peak current exhibited by tsA-201 cells expressing CaV1.2, CaVα2δ1 and CaVβ3 in the absence and presence of 4R0N-tau****. A) shows representative traces from a tsA201 cell when 4R0N-tau is absent, undergoing the protocol of pulses described in the methods section. B) shows representative traces from a tsA201 cell when 4R0N-tau is present, under the same conditions. C) shows a plot comparing average current at each voltage step of the protocol (control group n=22, control + 4R0N-tau n=26). D) shows an activation curve comparing the tau positive and negative groups. E shows time constant of decay in the range 0-+40 mV.*

As shown in Figure 6 the current size elicited in the control group and control + 4R0N-tau in the voltage range -10-50 mV is significantly different (p=0.0006). Figure 6D shows the activation curves generated from the control group and control + 4R0N-tau, for the control group V0.5 = -2.47 ±1.36 mV, for control + 4R0N-tau V0.5= -0.19 ±1.32 mV, there is no significant difference (p=0.8378). Figure 6E shows the decay rates from maximum current of the control group and control + 4R0N-tau group in the range 0-30 mV, there no significant

difference between the plots (p=0.1109). The presence of 4R0N-tau has no effect on the voltage dependence of activation or the current decay rates, this shows that the augmentation of Ca^{2+} currents is due to more channels being at the plasma membrane, rather than channel properties being altered.

4.3 Discussion

Overexpression of two out of three isoforms of 4R tau augments $Ca_v1.2$ LTCC currents (Stan et al., 2022), this augmentation was only seen when the pore forming subunit was co-expressed with Cavβ3 and not Cavβ2a (Stan et al., 2022). Figure 6 and previous experiments show that there is no significant difference in the activation curves and decay rates of $Ca_v1.2$ LTCC currents in these experiments, meaning that increase in current flow is due to a larger number of functional channels, not an increase in current flow through individual channels (Stan et al., 2022). Hence, $Ca_v1.2$ co-expressed with $Cav\beta_3$ was used in the experiments.

It is proposed that tau binds to $Ca_V\beta3$ and stabilizes L-type calcium channels in the membrane, increasing their number. This interaction is specific for certain tau isoforms (4R0N and 4R2N) that have a particular N-terminal repeat sequence that can interact with $Ca_V\beta3$ (Stan et al., 2022). This interaction is also specific for L-type calcium channels that have $Ca_V\beta3$ as their β subunit, which is more prevalent in certain brain regions, such as the hippocampus (Stan et al., 2022).

An accumulation of tau protein in the brain is a hallmark of several neurodegenerative diseases, such as AD and frontotemporal dementia. These diseases are also characterized by impaired cognition and memory, which depend on hippocampal function. It is possible that an excess of tau protein may increase the number and activity of L-type calcium channels in hippocampal neurons via its interaction with $Ca_V\beta3$, leading to increased calcium influx and AHPs. This may result in reduced neuronal excitability and plasticity, which may underlie the cognitive deficits observed in these diseases (Stan et al., 2022).

Figure 6 shows that presence of 4R0N-tau significantly increased the elicited currents from tsA201 cells expressing $Ca_v1.2$, α2δ1 and β_3 without changing the voltage dependence of activation or the rate of decay, agreeing with the literature (Stan et al., 2022). This implies that 4R0N-tau exerts this effect by increasing the number of functional LTCCs at the cell membrane or by stabilising the open conformation of LTCC, causing higher currents to be measured.

Chapter 5: Double Tryptophan mutation prevents LTCC expression.

5.1 Introduction

The β subunit of L-type calcium channels is an accessory subunit that modulates the function and expression of the α1 subunit, which forms the pore and the voltage sensor of the LTCC (Streissnig et al., 2014).

The β subunit has several roles in L-type calcium channels; increasing the peak calcium current by enhancing the channel opening probability and reducing the channel inactivation; shifting the voltage dependence of activation and inactivation to more negative potentials, making the channel more responsive to depolarization; modulating the G protein inhibition of the channel by interacting with the G β γ subunits and preventing their binding to the α1 subunit; controlling the α1 subunit membrane targeting by facilitating its trafficking from the endoplasmic reticulum to the plasma membrane and stabilizing it in the membrane (Buraei and Yang, 2013).

Commented [DS2]: Buraei and Yang, 2010 and Buraei and Yang, 2013 are listed in the reference list. Please select the correct reference

There are four isoforms of the beta subunit: β1, β2, β3, and β4. They have different expression patterns, binding affinities, and effects on LTCC function. For example, β1 and β2 are widely expressed in various tissues, while β3 and β4 are more restricted to certain brain regions. β1 and β3 have higher binding affinity for the α1 subunit than β2 and β4. β1 and β2 shift the voltage dependence of activation more than β3 and β4 (Striessing et al., 2014)

The β subunit connects to the α1 subunit through a conserved interaction domain (CID) located in the intracellular loop between domains I and II of the α1 subunit. The CID binds to a guanylate kinase (GK) domain in the C-terminal region of the β subunit. The GK domain is also involved in binding to other proteins, such as actin, tubulin, and spectrin, which may link the channel to the cytoskeleton (Shaw and Colecaft, 2013; Striessing et al., 2014).

Knockouts of different beta subunits of LTCCs have different effects on the channel activity and the physiology of various tissues and cells. Knockout of β1 in mice leads to severe cardiac dysfunction. The mice exhibit reduced L-type calcium currents and impaired excitation-contraction coupling, resulting in heart failure (Hofmann et al., 2014). Knockout of β2 in mice is also lethal at the embryo stage due to impaired cardiac development that is secondary to a decreased L-type calcium current. However, cardiac-specific excision of β2 in adult mice only moderately decreases L-type calcium current, suggesting that β2 may not be critical for α1C trafficking in adult ventricular myocytes (Dolphin, 2016). Knockout of β3 in mice does not

affect cardiac function but impairs long-term potentiation (LTP) and spatial learning in the hippocampus. This is linked to reduced expression and function of LTCC in hippocampal neurons (Shaw and Colecraft, 2013). Knockout of β4 in mice does not affect cardiac or hippocampal function but causes deafness and vestibular dysfunction. This is due to impaired expression and function of LTCCs in inner ear hair cells.

The genes that encode β subunits 1-4 of L-type calcium channels are called CACNB1, CACNB2, CACNB3, and CACNB4. These genes are located on chromosomes 17, 10, 12, and 2, respectively (Powers et al., 1992; Taviaux et al., 1997). The β subunits interact with the α-1 subunit of the channel, which is encoded by the CACNA1C gene, and modulate its expression and activity (Napolitano et al., 2006).

Alternative splicing is a process that allows a single gene to produce different versions of a protein by cutting and rearranging the genetic instructions in different ways (Liu et al., 2022). Alternative splicing of the CACNB genes can result in different isoforms of the β subunits, which have different effects on channel localisation and function. For example, one isoform of the β2 subunit, called β2a, has a shorter C-terminal region than another isoform, called β2e. This difference affects how the β-2 subunit interacts with the α-1 subunit and influences the channel's voltage sensitivity and kinetics.

Ca_Vβ3 has a modular structure, consisting of five main regions: the N-terminus, the SH3 domain, the HOOK region, the GK domain, and the C-terminus (Buraei and Yang, 2010). Each region has a specific function in regulating the channel activity and expression (Figure 7). The GK domain is a guanylate kinase-like domain that has no enzymatic activity but serves as a scaffold for protein-protein interactions. The GK domain of Ca_Vβ3 interacts with the α2δ subunit of the channel, which is another auxiliary subunit that enhances the membrane trafficking and expression of the α1 subunit. The GK domain also binds to a region in the α1 subunit called the α-interaction domain (AID), which is located on the intracellular loop between domains I and II. This interaction is crucial for stabilizing the α1 subunit and preventing its proteasomal degradation. The GK domain also modulates the voltage sensitivity and kinetics of the channel by altering the conformation of the α1 subunit (Buraei and Yang, 2013), shown in Figure 7.

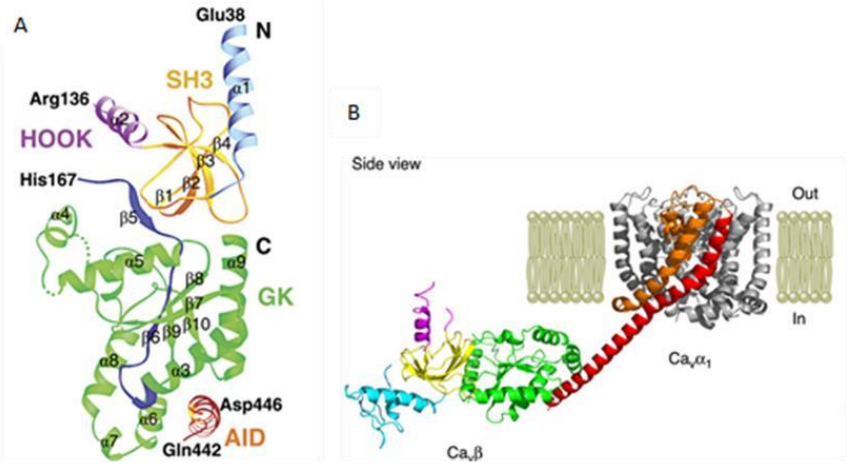

Figure 7 ***Crystal structures of Ca$_v$β3, AID and Ca$_v$α1*** *A) shows a crystal structure of the Ca$_v$β3 subunit in complex with the AID. The NH_2 terminus is shown in light blue, the SH3 domain in gold, the HOOK region in purple, the GK domain in green, the BID in dark blue and the AID in orange. B) shows the side view of a partial structural model of the Ca$_v$α1/Ca$_v$β complex. Only the S5 (shown in orange), P loop and S6 (shown in red) are shown in Ca$_v$α1. The AID linker (red) is shown as an alpha helix, joining with IS6 at the NH_2 terminus and the AID at its COOH terminus, the colours indicating the different domains and regions in Ca$_v$β are the same as in A. Adapted from Buraei and Yang, {2010}.*

Classic SH3 domains are small protein domains that can bind to proline-rich sequences in other proteins. They are involved in various cellular processes, such as signal transduction, cytoskeleton regulation, and endocytosis. SH3 domains have a β-barrel fold that consists of two anti-parallel β sheets with five or six β strands each (Lim et al., 1994; Larson & Davidson 2000). The Ca$_v$β SH3 domain has a similar fold to classical SH3 forms, but the last two β sheets are not continuous, as they are separated by the HOOK region (Chen et al., 2009). Ca$_v$β SH3 contains a well preserve PxxP binding motif, and so can bind to PxxP motif containing proteins. However, crystal structures of Ca$_v$β show that the HOOK region occludes the PxxP binding domain (Buraei and Yang, 2013). These crystal structures are taken of Cavβ without it being attached to a full length Ca$_v$α1 or other proteins, so it is possible that the HOOK region and loop may move to expose the PxxP binding site (Buraei and Yang, 2013).

Among the Ca$_v$β subfamilies, the HOOK region is variable in both length and sequence (Figure 8). In crystal structures, the HOOK region is largely unresolved due to poor electron density,

indicating it has as a high degree of flexibility (Buraei and Yang, 2013). This variability in the length of the HOOK region and its flexibility between isoforms of Cavβ could mean there is variability in occlusion of the hydrophobic residues between $Ca_v\beta$ subtypes.

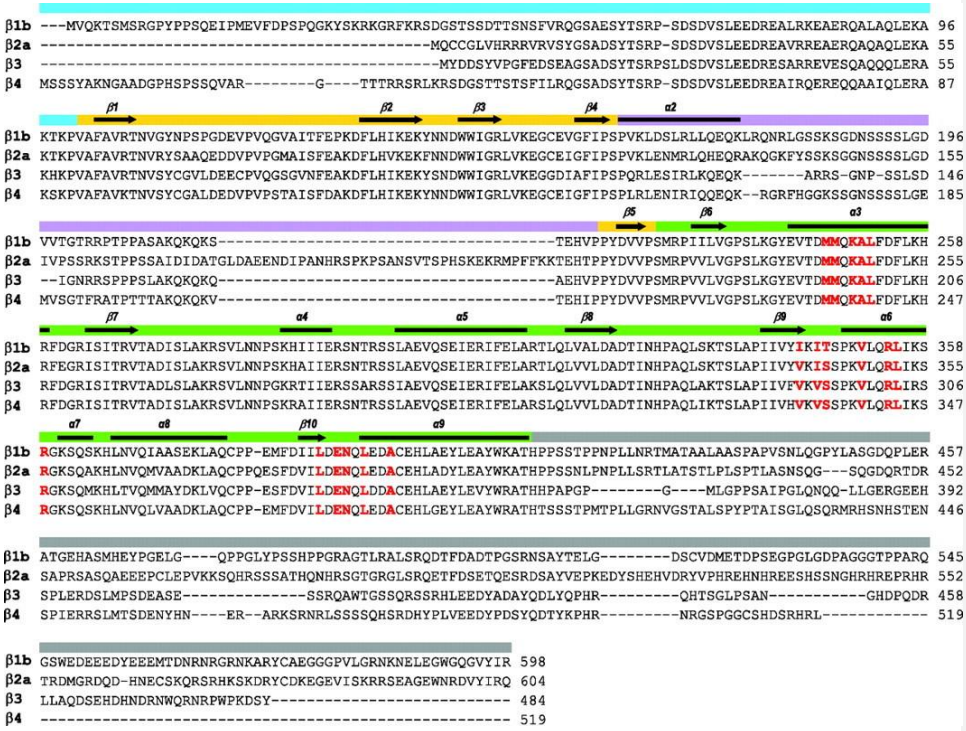

Figure 8 ***Amino acid sequence $Ca_v\beta$ subtypes, aligned****. The NH2 terminus is indicated by light blue, the SH3 domain by gold, the HOOK region by purple, The GK domain by green, and the COOH terminus by grey. Secondary structures are shown in the line above as arrows for β sheets and solid lines for α helices. Residues involved in interactions with the AID are in red. (Buraei & Yang 2010)*

The NH2 and COOH termini are highly variable in length and sequence (Figure 8). There is little known of the structure of the COOH terminus. However, the NH2 terminus of $Ca_v\beta4$ has been solved, revealing a fold consisting of two α helices and two antiparallel β sheets (Vendel et al., 2006).

The SH3 and GK domains interact intramolecularly (Chen et al., 2009). The affinity between the SH3 and GK domains is strong enough that hemi- $Ca_v\beta$ fragments containing SH3 and GK

modules can associate biochemically in vitro and regain their functionality in cells (Chen et al., 2009). The last β sheet of the SH3 domain, which is separated by the HOOK region, is critical for this interaction (Chen et al., 2009). It is directly connected to the GK domain and interacts with both the GK and SH3 domain (Chen et al., 2009), acting as a bridge to strengthen an otherwise weak interaction between the SH3 and GK domains (Chen et al., 2009). This interaction is important in the function of $Ca_v\beta$s (Chen et al., 2009), because weakening it by mutation or amino acid insertion severely compromises the gating effects of $Ca_v\beta$ (Chen et al., 2009). Therefore, any mutations that change the interaction between the SH3 and GK domains could produce significant functional consequences.

The linker between the $Ca_v\beta$ and $Ca_v1.2$ is a region in the intracellular loop between domains I and II of the Cav1.2 α1 subunit, which is the pore-forming subunit of the channel. This region is called the α-interaction domain (AID) and it is highly conserved among all high-voltage activated calcium channels (Pragnell et al., 1994). The AID interacts with the GK domain of the $Ca_v\beta$ subunit, which is a scaffold for protein-protein interactions. The AID-GK interaction is crucial for stabilizing the α1 subunit and preventing its proteasomal degradation. AID-GK interaction also modulates the voltage sensitivity and kinetics of the channel by altering the conformation of the α1 subunit. The AID is composed of 18 amino acids and has a helical structure. The GK domain has a groove that accommodates the AID helix. The interaction between the AID and GK is mainly mediated by hydrophobic and electrostatic interactions. The AID has three conserved residues that are essential for binding to the GK domain: a tryptophan at position 5, a phenylalanine at position 8, and an aspartate at position 10. These residues form a W-F-D motif that fits into a complementary pocket in the GK domain (Buraei and Yang, 2010).

The $Ca_v\beta$ SH3 domain was targeted for mutation due to its function in mediating protein-protein interactions through binding to PxxP motifs, following research that showed that mutation of residues in the second proline rich domain of 4R0N-tau abolishes the ability of 4R0N-tau to augment L-type calcium current (Withers, 2023). Tau has 2 proline rich domains, P1 and P2, so mutations in these regions are likely to affect tau binding (Figure 9).

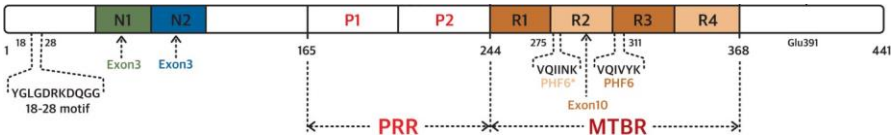

Figure 9 ***Scheme of tau showing domain organisation****. Depending on the isoform, tau can have an N-terminal extension with 0, 1, or 2 inserts (referred to as tau0N, tau1N, and tau2N, respectively). The presence of the N1 and N2 inserts is determined by exon 2 and exon 3, respectively. The microtubule-binding region (MTBR) contains either three (tau3R) or four (tau4R) repeats, with the presence of the R2 repeat depending on exon 10. The MTBR repeats, R1 to R4, each consist of 31 or 32 residues and have similar sequences. Adapted from Fichou et al. (2019).*

Commented [DS3]: The Figure legend is split over two pages. Please move Figure 9 and its legend to the next page (page 41). There is enough space for both Figures 9 and 10 and their legends

Commented [DS4]: This reference is missing from the list of references

Upon observing the crystal structure of $Ca_V\beta$, a potential binding pocket consisting of residues Y98, W102 and W103 was identified (Figure 10). Tryptophan is highly hydrophobic, and tyrosine has both hydrophobic and hydrophilic groups, suggesting that these residues might bind to proline rich tau. To test this hypothesis, a double mutation was designed, replacing both tryptophan residues W102 and W103 with two alanine residues AA.

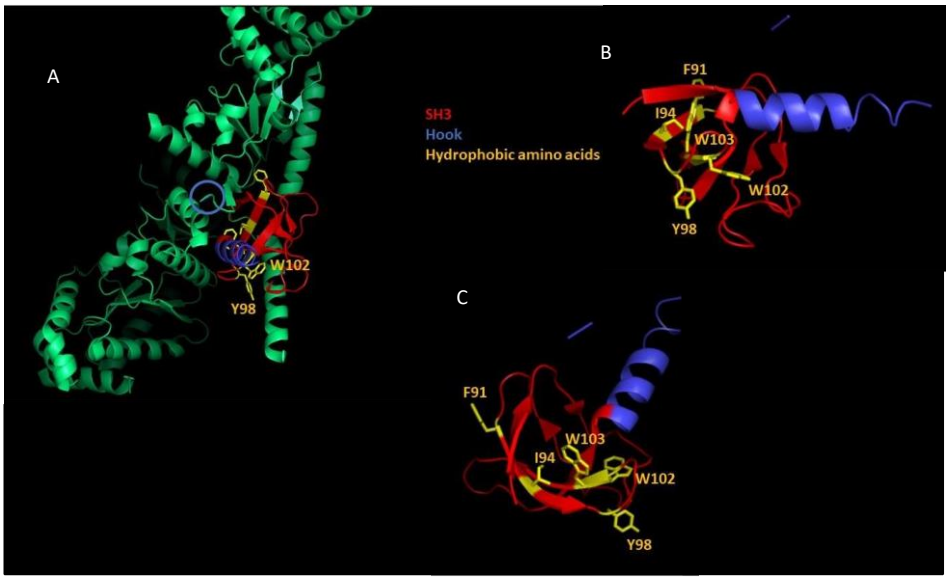

Figure 10 ***Molecular modelling of $Ca_V\beta_3$****. A) shows structure of $Ca_V\beta_3$ on larger scale, red shows SH3 domain, blue shows Hook region (blue circle shows where the Hook region re-joins the main structure) and yellow shows hydrophobic amino acids. B&C) Close up of hydrophobic amino acids. Image provided by Andrew Butler.*

5.2 Results

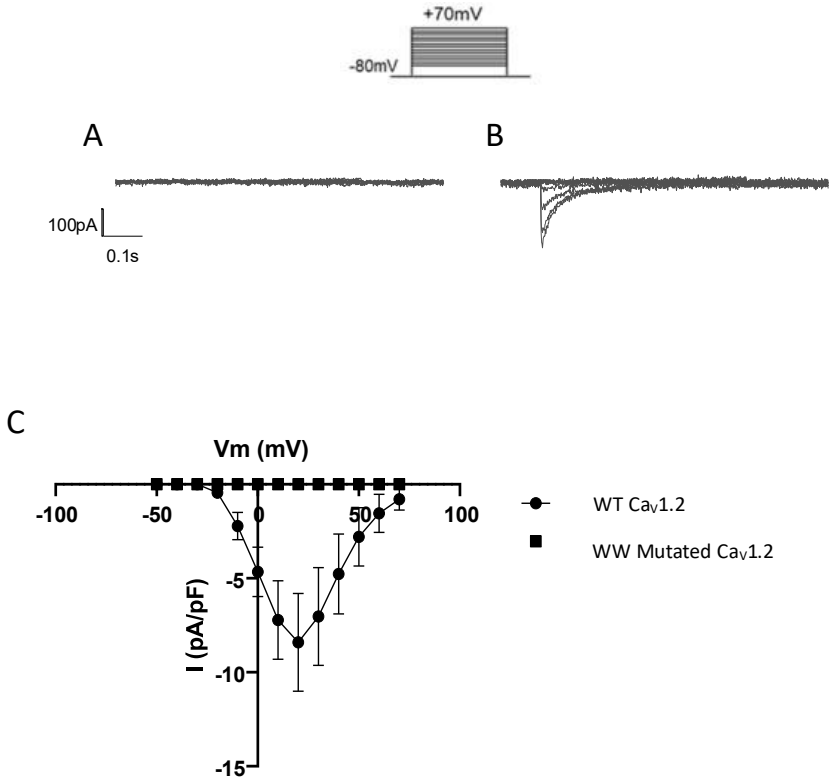

Figure 11 **The WW mutation prevents expression of LTCC** *A) representative trace from a tSA-201 cell exogenously expressing LTCCs with the WW mutation $Ca_v\beta 3$. B) shows a representative trace from a WT LTCC. C) shows an IV curve comparing WT and WW mutated currents* (n=15).

This experiment was carried out to assess the effect of the WW mutation in $Ca_v\beta 3$. tSA201 cells expressing the double tryptophan mutated β_3 did not express any current. The cells which underwent electrophysiological experimentation fluoresced when exposed to UV light, meaning they were expressing eGFP and the transfection was successful. This implies that the WW mutation prevented expression of LTCCs in the plasma membrane.

5.2 Discussion

Figure 11A and 11B compares representative traces from tsA201 cells expressing the WW β_3 mutation and WT β_3. This mutation removed the ability of the cells to express L-type currents. This could be due to the mutation changing the overall shape of the $Ca_v\beta3$ subunit, preventing it from functioning normally, meaning the LTCC will not have been trafficked to the cell membrane. This could be through interring with the intramolecular interaction between SH3 and GK which, as mentioned in chapter 5.1, is critical for $Ca_v\beta$ function, as tryptophan and tyrosine both play significant roles in protein folding.

Commented [DS5]: Please identify the section of your thesis that you are referring to

Chapter 6: Single point mutation of the double tryptophan motif in the $Ca_V\beta$ subunit prevents 4R0N-tau augmenting currents elicited by tsA-201 cells expressing LTCCs.

6.1 Introduction

The double tryptophan motif in the SH3 domain of *Caenorhabditis elegans* is essential for binding proline-rich domains (PRDs) of its target proteins. The double tryptophan motif consists of two conserved tryptophan residues that are separated by two or three amino acids and are located at the RT loop and the n-Src loop of the SH3 domain. These tryptophan residues form a hydrophobic pocket that accommodates the proline residues of the PRDs.

One example of an SH3 domain-containing protein in C. elegans is SEM-5, which is a homologue of human GRB2. SEM-5 has two SH3 domains, one at the N-terminus (SEM-5-NSH3) and one at the C-terminus (SEM-5-CSH3). SEM-5-NSH3 binds to PRDs with the PxxPxR core motif, while SEM-5-CSH3 binds to PRDs with the PxxxRxxKP core motif (Harkiolaki et al., 2003).

The double tryptophan motif is essential for both SEM-5-NSH3 and SEM-5-CSH3 to bind to their respective PRDs. Mutations of either tryptophan residue in the double tryptophan motif significantly reduce or abolish the binding affinity and specificity of the SH3 domains (Lim et al., 1994). Therefore, we generated a Cavβ3 mutant where the first tryptophan is replaced by phenylalanine (W102F).

6.2 Results

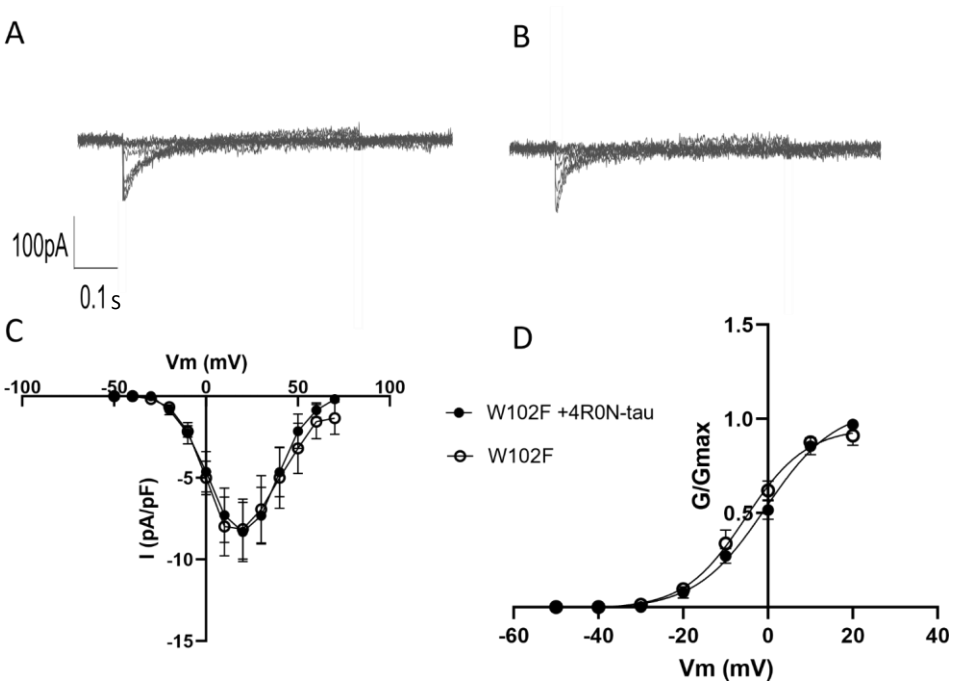

Figure 12 **The W102F mutation removes the effect of 4R0N-tau augmenting LTCCs**. *A) shows a representative trace from a tsA201 cell expressing $Ca_v1.2$, α2δ1 and W102FCaVβ$_3$, B shows a representative trace from a tsA201 cell expressing the subunits with 4R0N-tau also expressed. C shows IV curves comparing W102F tsA201 cells alone* (n=11) *and in the presence of tau* (n=9)*. D shows the activation curves of W102FCaVβ$_3$ and W102FCaVβ$_3$+4R0N-tau.*

Figure 12 shows representative families of currents (Figure 12 A and B) and the IV curves generated from currents elicited from tsA201 cell expressing $Ca_v1.2$, α2δ1 and W102FCaVβ$_3$ with and without 4R0N-tau expressed (Figure 12C). There is no significant different between the curves (p=0.5469)

Figure 12D compares the activation curves generated for W102F (V0.5= -2.04±1.16 mV) and for W102F+4R0N-tau (V0.5= 0.21±1.70 mV). There was no significant difference (p=0.9192). There is also no significant difference between these V0.5 and the V0.5 values gathered from tsA201 cells expressing WT β$_3$ (V0.5 = -2.47 ±1.36 mV) and WT+4R0N-tau (V0.5= -0.19 ±1.32 mV) (p=0.9938).

When comparing the currents elicited from WT $Ca_V1.2$ with W102F $Ca_V\beta_3$. No significant difference was found (p=0.8839).

6.3 Discussion

Figure 12 shows that when the W102F mutation is expressed in tsA201 cells, the augmentation of current flow due to 4R0N-tau seen in Figure 6 was not present. These results imply that as in the *Caenorhabditis elegans* protein SEM-5 and its human and *Drosophila* homologues, Grb2 and Drk, the first tryptophan is essential for binding to the proline rich domains in 4R0N-tau. However, it does not exclude the possibility that residue W103F in the $Ca_v\beta3$ subunit contributes to the interaction between 4R0N-tau and $Ca_v\beta3$. Tau has 7 PxxP motifs in two proline rich regions (P1 and P2).

I hypothesise that the WW102-3 motif in LTCCs strongly interacts with one of the PxxP motifs in 4R0N-tau, stabilising the LTCC at the cell membrane, increasing the number of channels present in the membrane and so, increasing Ca^{2+} entry. Tryptophan, and phenylalanine are structurally and chemically similar, so this is a very specific interaction. I hypothesise that the specific combination of the shape and strength of hydrophobicity are essential for this interaction.

Previous reports have shown that the current enhancement by 4R0N-tau is only observed when the calcium channel contains the $Ca_v\beta_3$ subunit, and not with the $Ca_v\beta_{2a}$ subunit (Stan et al., 2022). I propose that this is due to the different lengths of HOOK regions in these isoforms. Figure 13 shows the amino acid sequence of both $Ca_v\beta3$ and $Ca_v\beta2a$ aligned. The HOOK region in the $Ca_v\beta_{2a}$ subunit is twice as long (98 amino acids) as $Ca_v\beta3$ (49 amino acids). I propose that the longer HOOK region in $Ca_v\beta2a$ occludes the WW102-3 binding site, preventing tau from binding, hence stopping the augmentation of current flow seen in $Ca_v\beta3$, explaining the subunit specificity of this interaction. $Ca_v\beta3$ is also expressed with $Ca_V2.1$ and 2.2, but there is no evidence that the function of either of these alpha subunits changes in age or tauopathy.

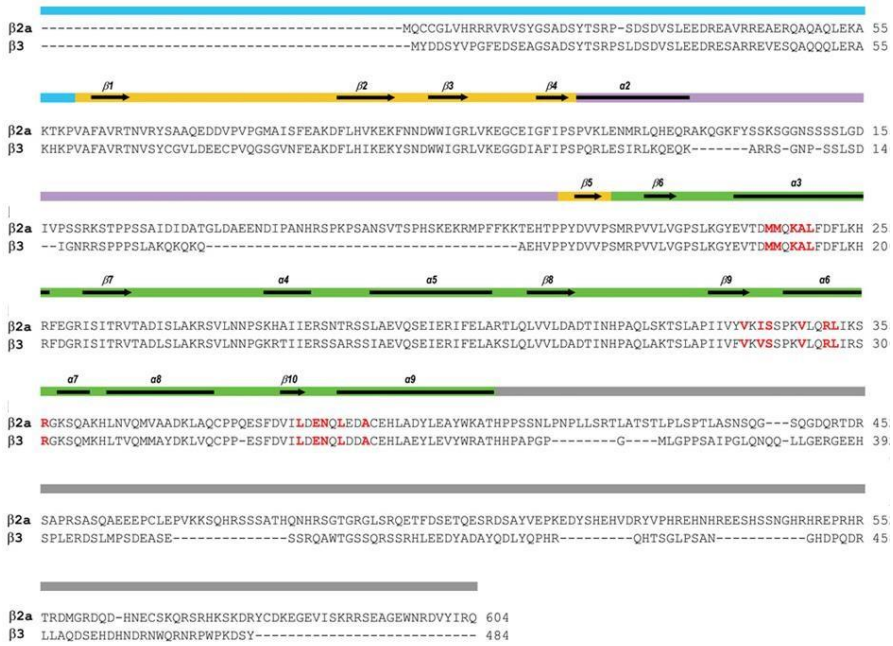

Figure 13 ***Aligned amino acid sequence of β2a (GenBank accession number, M80545) and β3 (M88751)****. Light blue indicated the NH2 terminus, gold the SH3 domain, purple the HOOK region, green the GK region, and grey the COOH terminus. Secondary structures are shown in the line above as arrows for β sheets and solid lines for α helices. Residues involved with the AID are marked in red. Edited from Buraei & Yang 2010.*

Chapter 7: General Discussion

The exact mechanisms behind tauopathies are still not fully understood, but several hypotheses have been proposed.

Loss of function, this hypothesis suggests that when tau detaches from the microtubules, it reduces its stability, affecting its ability to transport molecules and organelles within neurons. This leads to impaired neuronal communication and degeneration (Chung et al., 2021; Zhang et al., 2022b).

Gain of function, this hypothesis suggests that the abnormal tau aggregates have toxic effects on neurons, such as triggering inflammation, oxidative stress, mitochondrial dysfunction, calcium dysregulation, and apoptosis. These effects may also spread to neighbouring cells through a process called prion-like propagation, where misfolded tau acts as a seed that induces more tau aggregation (Chung et al., 2021; Silva et al., 2020).

Mislocalisation, this hypothesis suggests that hyperphosphorylated tau is abnormally transported from the axons to other parts of neurons, such as the dendrites and the soma. This disrupts the normal polarity and signalling of neurons and may also interfere with other cellular functions, such as gene expression, synaptic plasticity, and autophagy (Chung et al., 2021; Zhang et al., 2022b).

The different hypotheses to explain tauopathies are not mutually exclusive and may interact with each other in complex ways. Moreover, different tauopathies may have different predominant mechanisms depending on the type, location, and conformation of tau aggregates. For example, AD is characterized by both neuronal and glial tau pathology, while some primary tauopathies have mainly glial involvement. Also, different tau isoforms may have different propensities to aggregate and different effects on neuronal function. For instance, 3R tau is more abundant in foetal brains, while 4R tau is more prevalent in adult brains. Some tauopathies have a balanced ratio of 3R and 4R tau, while others have an imbalance that favours one over the other (Silva et al., 2020; Chung et al., 2021).

To better understand the mechanisms behind tauopathies, researchers have used various methods and tools, such as mouse models, induced pluripotent stem cells, transcriptomics, and cryo-electron microscopy. These approaches have helped reveal some of the molecular and cellular details of tau pathology and its consequences for brain function. However, there are still many challenges and limitations that need to be overcome, such as replicating the human disease phenotypes in animal models, identifying reliable biomarkers for diagnosis

and prognosis, and developing effective therapies that can target tau aggregation and its downstream effects (Silva et al., 2020; Chung et al., 2021; Zhang et al., 2022a).

This research is a continuation of the work described in Stan et al., (2022) and Withers (2023), which showed tau isoform specific enhancement of LTCC current and the interaction site within 4R0N-tau and LTCCs, respectively. In this research a point mutation has been identified in the $Ca_V\beta3$ subunit which prevents the effect of 4R0N-tau augmenting L type calcium currents. This is significant as this effect could cause greater spike frequency adaptation through augmentation of the calcium dependent component of medium and slow AHPs. Spike frequency adaptation is when the frequency of action potentials decreases over time when a constant stimulus is applied, an increase in adaption through augmented medium and slow AHPs would stop cells firing as frequently as they normally would in response to a stimulus, which could explain cognitive decline seen in early AD and tauopathies.

The effect of tau augmenting L type currents could accumulate over many years. With neurons having greater than normal calcium entry for an extended period putting strain on the neurons to maintain intracellular calcium levels at around 100 nM until the cell can no longer maintain normal calcium homeostasis, and intracellular calcium concentration increases. Intracellular calcium is known to be increased in AD and tauopathies (Scheltens et al., 2016). For example, the intracellular calcium level within cortical neurons of a mouse transgenic model of AD (3xTg-AD) was found to be twice that observed in normal cortical neurons (Sterniczuk et al., 2010). Increased intracellular calcium will cause excitotoxic injury and kill the cells, leaving the neurofibrillary tangles of tau seen in dementia brains. The cell death could also release soluble tau into the extracellular space which would explain the presence of 4R0N-tau in cerebrospinal fluid of AD patients (Carlomagno et al., 2021). Extracellular 4R2N -tau has been shown to interact with M1 and M3 muscarinic receptors, promoting an increase in intracellular calcium (Medina & Avila, 2014), this could be a mechanism of cell death spreading to neighbouring cells.

Interestingly, the effect seen here is like the effect seen in the calcium hypothesis of brain aging, where cognitive decline is seen even in the absence of any detectable dementias. This dysfunction occurs mainly in the hippocampus before spreading to the neocortex. Historically, this was thought to be due to neuronal loss (Mani et al., 1986), but this was refuted when significant cell death was not found in the hippocampus in normal aged brains (Rapp and Gallagher, 1996). In hippocampal neurons biophysical properties such as input

resistance, resting membrane potential, and membrane time constant are preserved in aged brains (Burke and Barnes 2006). Dysregulation of postsynaptic firing is a likely cause of age-related cognitive decline, which is dependent on correct calcium homeostasis. Intracellular calcium concentration, calcium dependent potassium conductance and AHPs are all increased in aging brains (Landfield and Pitler, 1984; Khachaturian, 1989). Excessive calcium flow through LTCCs contribute to all these factors.

The interaction between 4R0N-tau and LTCCs characterised in this research causes the same effect as described in the Calcium Hypothesis of brain aging. This could imply that perhaps dementia is an acceleration of the normal aging process though dysregulation of calcium flow through LTCCs.

The data gathered in this research combined with those of Stan et al., (2022) and Withers (2023) thesis provide a possible novel mechanism for the cognitive decline seen in tauopathies, which contribute to the issues of identifying reliable biomarkers for prognosis, and developing effective therapies that can target tau aggregation and its downstream effects. However, it is unlikely that this interaction between 4R0N-tau and LTCCs is the only mechanism behind tauopathies. It is more likely to be a combination of mechanisms and hypotheses, one of the limitations of this research is that it is performed with cell lines, and while this allowed us to isolate the channel, it also prevents us from being able to see how it interacts with wider systems. To extend this research, it could be carried out in more complex models e.g. brain slices. Alternatively, a small molecule could be designed which competes for either or both the 4R0N-tau and $Ca_V\beta3$ binding sites. This could be compared to the effect of nimodipine in cell lines and mouse models to explore whether the small molecule rescues disease progression.

To conclude, point mutation of the W102F residue in $Ca_V\beta3$ removes the effect of 4R0N-tau augmenting L-type currents in tsA201 cells. However, it is possible the W103F residue is also involved in this effect. This evidence along with results detailed in Stan et al., (2022) and Withers (2023) shows that 4R0N-tau interacts with the $Ca_V\beta3$ subunit of LTCCs and provides a potential novel mechanism of AD and potential therapeutic target for further study in more complex models for cognitive decline seen in AD and tauopathies

References

Avila, J., Jimenez, J.S., Sayas, C.L., Bolos, M., Zabala, J.C., Rivas, G. and Hernandez, F., 2016. Tau Structures. *Frontiers in Aging Neuroscience*, 8, p.262. doi: 10.3389/fnagi.2016.00262.

Bannister, J.P., Leo, M.D., Narayanan, D., Jangsangthong, W., Nair, A., Evanson, K.W., Pachau, J., Gabrick, K.S., Boop, F.A. and Jaggar, J.H., 2013. The voltage-dependent L-type Ca^{2+} ($Ca_v1.2$) channel C-terminus fragment is a bi-modal vasodilator. *Journal of Physiology*, 591(12), pp.2987-2998.

Boda, D., Valisko, M., Henderson, D., Eisenberg, B., Gillespie, D. and Nonner, W., 2009. Ionic selectivity in L-type calcium channels by electrostatics and hard-core repulsion. *Journal of General Physiology*, 133(5), pp.497-509. doi: https://doi.org/10.1085/jgp.200910211.

Bodi, I., Mikala, G., Koch, S.E., Akhter, S.A. and Schwartz, A., 2005. The L-type calcium channel in the heart: the beat goes on. *Journal of Clinical Investigation*, 115, pp.3306-3317.

Bourinet, E. and Zamponi, G.W., 2017. Block of voltage-gated calcium channels by peptide toxins. *Neuropharmacology*, 127, pp.109-115.

Buchholz, S. and Zempel, H. 2024. The six brain-specific TAU isoforms and their role in Alzheimer's disease and related neurodegenerative dementia syndromes. *Alzheimer's & Dementia: the journal of the Alzheimer's Association, 20(5), pp 3606-3628.*

Buraei, Z. and Yang, J., 2010. The ß subunit of voltage-gated Ca^{2+} channels. *Physiological Reviews*, 90, pp.1461-1506.

Buraei, Z. and Yang, J., 2013. Structure and function of the β subunit of voltage-gated Ca^{2+} channels. *Biochimica et Biophysica Acta*, 1828, pp.1530-1540.

Burke, S.N. and Barnes, C.A., 2006. Neural plasticity in the ageing brain. *Nature Reviews Neuroscience*, 7(1), pp.30-40. doi: 10.1038/nrn1809.

Cain, S.M. and Snutch, T.P., 2011. Voltage-gated calcium channels and disease. *Biofactors*, 37(3), pp.197-205. doi: 10.1002/biof.158.

Calderon-Rivera, A., Andrade, A., Hernandez-Hernandez, O., Gonzalez-Ramirez, R., Sandoval, A., Rivera, M., Gomora, J.C. and Felix, R., 2012. Identification of a disulfide bridge essential for structure and function of the voltage-gated Ca^{2+} channel α2δ-1 auxiliary subunit. *Cell Calcium*, 51, pp.22-30.

Carlomagno, Y., Manne, S., DeTure, M., Prudencio, M., Zhang, Y.J., Al-Shaikh, R.H., Dunmore, J.A., Daughrity, L.M., Song, Y., Castanedes-Casey, M., Lewis-Tuffin, L.J., Nicholson, K.A., Wszolek, Z.K., Dickson, D.W., Fitzpatrick, A.W.P., Petrucelli, L. and Cook, C.N.,

2021. The AD tau core spontaneously self-assembles and recruits full-length tau to filaments. *Cell Reports*, 34(11), p.108843. doi: 10.1016/j.celrep.2021.108843.

Carlson, A.P., Hänggi, D., Macdonald, R.L. and Shuttleworth, C.W., 2020. Nimodipine Reappraised: An Old Drug with a Future. *Current Neuropharmacology*, 18(1), pp.65-82. doi: 10.2174/1570159X17666190927113021.

Catterall, W.A., 2011. Voltage-gated calcium channels. *Cold Spring Harbor Perspectives in Biology*, 3(8), p.a003947. doi: 10.1101/cshperspect.a003947.

Chen, H., Zhang, D., Hua Ren, J. and Ping Chao, S., 2013. Effects of L-type Calcium Channel Antagonists Verapamil and Diltiazem on fKv1.4ΔN Currents in Xenopus oocytes. *Iranian Journal of Pharmaceutical Research*, 12(4), pp.855-866.

Chen, Y.H., He, L.L., Buchanan, D.R., Zhang, Y., Fitzmaurice, A. and Yang, J., 2009. Functional dissection of the intramolecular Src homology 3-guanylate kinase domain coupling in voltage-gated Ca^{2+} channel beta-subunits. *FEBS Letters*, 583(12), pp.1969-1975. doi: 10.1016/j.febslet.2009.05.001.

Cheng, S.H., Rich, D.P., Marshall, J., Gregory, R.J., Welsh, M.J. and Smith, A.E., 1991. Phosphorylation of the R domain by cAMP-dependent protein kinase regulates the CFTR chloride channel. *Cell*, 66(5), pp.1027-1036. doi: 10.1016/0092-8674(91)90446-6.

Chung, C.C., Chan, L., Chen, J.H., Bamodu, O.A., Chiu, H.W. and Hong, C.T., 2021. Plasma extracellular vesicles tau and β-amyloid as biomarkers of cognitive dysfunction of Parkinson's disease. *FASEB Journal*, 35(10), p.e21895. doi: 10.1096/fj.202100787R.

Coulon, P., 2021. Electrophysiological and Calcium Imaging Approaches to Study Metabotropic Glutamate Receptors. In: Olive, M.F., Burrows, B.T. and Leyrer-Jackson, J.M. (eds) *Metabotropic Glutamate Receptor Technologies*. Neuromethods, vol 164. Humana, New York, NY. doi: 10.1007/978-1-0716-1107-4_4.

Cui, G., Cottrill, K.A. and McCarty, N.A., 2021. Electrophysiological Approaches for the Study of Ion Channel Function. In: Schmidt-Krey, I. and Gumbart, J.C. (eds) *Structure and Function of Membrane Proteins*. Methods in Molecular Biology, vol 2302. Humana, New York, NY. doi: 10.1007/978-1-0716-1394-8_4.

Denning, G.M., Anderson, M.P., Amara, J.F., Marshall, J., Smith, A.E. and Welsh, M.J., 1992. Processing of mutant cystic fibrosis transmembrane conductance regulator is temperature sensitive. *Nature*, 358(6389), pp.761-764. doi: 10.1038/358761a0.

Disterhoft, J.F., Thompson, L.T., Moyer, J.R. Jr. and Mogul, D.J., 1996. Calcium-dependent afterhyperpolarization and learning in young and aging hippocampus. *Life Sciences*, 59, pp.413-420.

Dolphin, A.C., 2016. Voltage-gated calcium channels and their auxiliary subunits: physiology and pathophysiology and pharmacology. *Journal of Physiology*, 594(19), pp.5369-5390. doi: 10.1113/JP272262.

Dwivedi, D. and Bhalla, U.S., 2021. Physiology and Therapeutic Potential of SK, H, and M Medium AfterHyperPolarization Ion Channels. *Frontiers in Molecular Neuroscience*, 14, p.658435. doi: 10.3389/fnmol.2021.658435.

Fan, J.S., Yuan, Y. and Palade, P., 2001. FPL-64176 modifies pore properties of L-type Ca^{2+} channels. *American Journal of Physiology-Cell Physiology*, 280(3), pp.C565-C572.

Faber, E.S. and Sah, P., 2007. Functions of SK channels in central neurons. *Clinical and Experimental Pharmacology and Physiology*, 34, pp.1077-1083.

Feng, T., Kalyaanamoorthy, S. Barakat, K., Shad, KF. 2018. L-Type Calcium Channels: Structure and Functions. In: *Ion Channels in Health and Sickness*. IntechOpen. doi: 10.5772/intechopen.77305.

Fichou Y, Al-Hilaly YK, Devred F, Smet-Nocca C, Tsvetkov PO, Verelst J, Winderickx J, Geukens N, Vanmechelen E, Perrotin A, Serpell L, Hanseeuw BJ, Medina M, Buée L, Landrieu I. 2019. The elusive tau molecular structures: can we translate the recent breakthroughs into new targets for intervention? Acta Neuropathologica Communications .7(1) pp 31.

Fozzard, H.A., 2002. Cardiac sodium and calcium channels: a history of excitatory currents. *Cardiovascular Research*, 55(1), pp.1-8. doi: 10.1016/S0008-6363(02)00407-8.

Fox, A.P., Nowycky, M.C. and Tsien, R.W., 1987. Single-channel recordings of three types of calcium channels in chick sensory neurones. *Journal of Physiology*, 394, pp.173-200. doi: 10.1113/jphysiol.1987.sp016865.

Guo, T., Noble, W. and Hanger, D.P., 2017. Roles of tau protein in health and disease. *Acta Neuropathologica*, 133(5), pp.665-704. doi: 10.1007/s00401-017-1707-9.

Harkiolaki, M., Lewitzky, M., Gilbert, R.J., Jones, E.Y., Bourette, R.P., Mouchiroud, G., Sondermann, H., Moarefi, I. and Feller, S.M., 2003. Structural basis for SH3 domain-mediated high-affinity binding between Mona/Gads and SLP-76. *The EMBO Journal*, 22(11), pp.2571-2582. doi: 10.1093/emboj/cdg258.

Higham, J., Sahu, G., Wazen, R.M., Colarusso, P., Gregorie, A., Harvey, B.S.J., Goudswaard, L., Varley, G., Sheppard, D.N., Turner, R.W. and Marrion, N.V., 2019. Preferred Formation of

Commented [DS6]: This book chapter is missing the editor of the book

Heteromeric Channels between Coexpressed SK1 and IKCa Channel Subunits Provides a Unique Pharmacological Profile of Ca2±Activated Potassium Channels. *Molecular Pharmacology*, 96(1), pp.115-126. doi: 10.1124/mol.118.115634.

Hofmann, F., Flockerzi, V., Kahl, S. and Wegener, J.W., 2014. L-type $Ca_v1.2$ calcium channels: from in vitro findings to in vivo function. *Physiological Reviews*, 94, pp.303-326. doi: 10.1152/physrev.00016.2013.

Hullin, R., Khan, I.F., Wirtz, S., Mohacsi, P., Varadi, G., Schwartz, A. and Herzig, S., 2003. Cardiac L-type calcium channel beta-subunits expressed in human heart have differential effects on single channel characteristics. *Journal of Biological Chemistry*, 278(24), pp.21623-21630. doi: 10.1074/jbc.M211164200.

Iqbal, K., Liu, F., Gong, C.X. and Grundke-Iqbal, I., 2010. Tau in Alzheimer disease and related tauopathies. *Current Alzheimer Research*, 7(8), pp.656-664. doi: 10.2174/156720510793611592.

Johnson, G.V. and Jenkins, S.M., 1999. Tau protein in normal and Alzheimer's disease brain. *Journal of Alzheimer's Disease*, 1(4-5), pp.307-328. doi: 10.3233/jad-1999-14-511.

Kang, M.G. and Campbell, K.P., 2003. γ Subunit of Voltage-activated Calcium Channels. *Journal of Biological Chemistry*, 278(24), pp.21315-21318. doi: https://doi.org/10.1074/jbc.R300004200.

Khachaturian, Z.S., 1989. Calcium, membranes, aging, and Alzheimer's disease. Introduction and overview. *Annals of the New York Academy of Sciences*, 568, pp.1-4. doi: 10.1111/j.1749-6632.1989.tb12485.x.

Kovacs, G.G., 2017. Tauopathies. *Handbook of Clinical Neurology*, 145, pp.355-368. doi: 10.1016/B978-0-12-802395-2.00025-0.

Kubalova, Z., 2003. Inactivation of L-type calcium channels in cardiomyocytes. Experimental and theoretical approaches. *General Physiology and Biophysics*, 22(4), pp.441-454.

Landfield, P.W. and Pitler, T.A., 1984. Prolonged Ca^{2+} dependent afterhyperpolarizations in hippocampal neurons of aged rats. *Science*, 226(4678), pp.1089-1092. doi: 10.1126/science.6494926.

Larson, S.M. and Davidson, A.R., 2000. The identification of conserved interactions within the SH3 domain by alignment of sequences and structures. *Protein Science*, 9, pp.2170-2180.

Lehmann-Horn, F. and Jurkat-Rott, K., 1999. Voltage-gated ion channels and hereditary disease. *Physiological Reviews*, 79(4), pp.1317-1372. doi: 10.1152/physrev.1999.79.4.1317.

Lim, W.A., Richards, F.M. and Fox, R.O., 1994. Structural determinants of peptide-binding orientation and of sequence specificity in SH3 domains. *Nature*, 372, pp.375-379.

Lima, P.A. and Marrion, N.V., 2007. Mechanisms underlying activation of the slow AHP in rat hippocampal neurons. *Brain Research*, 1150, pp.74-82.

Lipscombe, D., Helton, T.D. and Xu, W., 2004. L-Type Calcium Channels: The Low Down. *Journal of Neurophysiology*, 92(5), pp.2633-2641.

Liu, S., 2024. Electrophysiological Methods to Measure Ca^{2+} Current. In: Liu, S. (ed.) *Rheumatoid Arthritis*. Methods in Molecular Biology, vol 2766. Humana, New York, NY. https://doi.org/10.1007/978-1-0716-3682-4_21.

Liu, Q., Fang, L. and Wu, C., 2022. Alternative Splicing and Isoforms: From Mechanisms to Diseases. *Genes (Basel)*, 13(3), p.401. doi: 10.3390/genes13030401.

Mandelkow, E., von Bergen, M., Biernat, J. and Mandelkow, E.M., 2007. Structural principles of tau and the paired helical filaments of Alzheimer's disease. *Brain Pathology*, 17(1), pp.83-90. doi: 10.1111/j.1750-3639.2007.00053.x.

Mani, R., Lohr, J. and Jeste, D., 1986. Hippocampal pyramidal cells and aging in the human: a quantitative study of neuronal loss in sectors CA1 to CA4. *Experimental Neurology*, 94, pp.29-40.

Manz, K.M., Siemann, J.K., McMahon, D.G. and Grueter, B.A., 2021. Patch-clamp and multi-electrode array electrophysiological analysis in acute mouse brain slices. *STAR Protocols*, 2(100442). doi: https://doi.org/10.1016/j.xpro.2021.100442.

Marrion, N.V. and Tavalin, S.J., 1998. Selective activation of Ca^{2+} activated K^{+} channels by co-localized Ca2+ channels in hippocampal neurons. *Nature*, 395(6705), pp.900-905. doi: 10.1038/27674.

Matthews, E.A., Linardakis, J.M. and Disterhoft, J.F., 2009. The Fast and Slow Afterhyperpolarizations Are Differentially Modulated in Hippocampal Neurons by Aging and Learning. *The Journal of Neuroscience*, 29, p.4750.

Medina, M. and Avila, J., 2014. New perspectives on the role of tau in Alzheimer's disease. Implications for therapy. *Biochemical Pharmacology*, 88(4), pp.540-547. doi: 10.1016/j.bcp.2014.01.013.

Moore, S.G. and Murphy, G.G., 2020. The role of L-type calcium channels in neuronal excitability and aging. *Neurobiology of Learning and Memory*, 173, p.107230. doi: https://doi.org/10.1016/j.nlm.2020.107230.

Morales, D., Hermosilla, T. and Vaela, D., 2019. Calcium-dependent inactivation controls cardiac L-type Ca^{2+} currents under β-adrenergic stimulation. *Journal of General Physiology*, 151(6), pp.786-797. doi: https://doi.org/10.1085/jgp.201812236.

Moyer, J.R. Jr., Thompson, L.T., Black, J.P. and Disterhoft, J.F., 1992. Nimodipine increases excitability of rabbit CA1 pyramidal neurons in an age- and concentration-dependent manner. *Journal of Neurophysiology*, 68, pp.2100-2109.

Nanou, E., Lee, A. and Catterall, W.A., 2018. Control of Excitation/Inhibition Balance in a Hippocampal Circuit by Calcium Sensor Protein Regulation of Presynaptic Calcium Channels. *Journal of Neuroscience*, 38(18), pp.4430-4440. doi: 10.1523/JNEUROSCI.0022-18.2018.

Napolitano, C., Timothy, K.W., Bloise, R. and Priori, S.G., 2006 [updated 2021]. CACNA1C-Related Disorders. In: Adam, M.P., Feldman, J., Mirzaa, G.M., Pagon, R.A., Wallace, S.E., Bean, L.J.H., Gripp, K.W. and Amemiya, A., eds. *GeneReviews® [Internet]*. Seattle (WA): University of Washington, Seattle; 1993–2024.

Patel, R. and Dickenson, A.H., 2016. Mechanisms of the gabapentinoids and α2δ-1 calcium channel subunit in neuropathic pain. *Pharmacology Research & Perspectives*, 4(2), p.e00205. doi: 10.1002/prp2.205.

Pei, Z.M., Murata, Y., Benning, G., Thomine, S., Klüsener, B., Allen, G.J., Grill, E. and Schroeder, J.I., 2000. Calcium channels activated by hydrogen peroxide mediate abscisic acid signalling in guard cells. *Nature*, 406(6797), pp.731-734. doi: 10.1038/35021067.

Power, J.M., Wu, W.W., Sametsky, E., Oh, M.M. and Disterhoft, J.F., 2002. Age-related enhancement of the slow outward calcium-activated potassium current in hippocampal CA1 pyramidal neurons in vitro. *Journal of Neuroscience*, 22, pp.7234-7243.

Powers, P.A., Liu, S., Hogan, K. and Gregg, R.G., 1992. Skeletal muscle and brain isoforms of a beta-subunit of human voltage-dependent calcium channels are encoded by a single gene. *Journal of Biological Chemistry*, 267(32), pp.22967-22972.

Pragnell, M., De Waard, M., Mori, Y., Tanabe, T., Snutch, T.P. and Campbell, K.P., 1994. Calcium channel β-subunit binds to a conserved motif in the I-II cytoplasmic linker of the α1-subunit. *Nature*, 368(6466), pp.67-70. doi: 10.1038/368067a0.

Qin, N., Yagel, S., Momplaisir, M.L., Codd, E.E. and D'Andrea, M.R., 2002. Molecular cloning and characterization of the human voltage-gated calcium channel α2δ-4 subunit. *Molecular Pharmacology*, 62(3), pp.485-496. doi: https://doi.org/10.1124/mol.62.3.485.

Rapp, P.R. and Gallagher, M., 1996. Preserved neuron number in the hippocampus of aged rats with spatial learning deficits. *Proceedings of the National Academy of Sciences of the United States of America*, 93(18), pp.9926-9930. doi: 10.1073/pnas.93.18.9926.

Robinson, P., 2011. Targeting of Voltage-Gated Calcium Channels to Lipid Rafts: The Role of Auxiliary α2/δ-1 Subunits. *PhD Thesis*. University of Manchester.

Rosenthal, J., 1994. Nilvadipine: profile of a new calcium antagonist. An overview. *Journal of Cardiovascular Pharmacology*, 24(Suppl 2), pp.S92-S107.

Sahu, G. and Turner, R.W., 2021. The molecular basis for the calcium-dependent slow afterhyperpolarization in CA1 hippocampal pyramidal neurons. *Frontiers in Physiology*, 12, p.759707. doi: 10.3389/fphys.2021.759707.

Scheltens, P., Blennow, K., Breteler, M.M., de Strooper, B., Frisoni, G.B., Salloway, S. and Van der Flier, W.M., 2016. Alzheimer's disease. *The Lancet*, 388(10043), pp.505-517. doi: 10.1016/S0140-6736(15)01124-1.

Schoch, K.M., DeVos, S.L., Miller, R.L., Chun, S.J., Norrbom, M., Wozniak, D.F., Dawson, H.N., Bennett, C.F., Rigo, F. and Miller, T.M., 2016. Increased 4R-Tau induces pathological changes in a human-tau mouse model. *Neuron*, 90, pp.941-947. doi: 10.1016/j.neuron.2016.04.042.

Shaw, R.M. and Colecraft, H.M., 2013. L-type calcium channel targeting and local signalling in cardiac myocytes. *Cardiovascular Research*, 98, pp.177-186. doi: 10.1093/cvr/cvt021.

Sheppard, D.N., 2011. Cystic Fibrosis: CFTR Correctors to the Rescue. *Chemistry & Biology*, 18 , pp.145-147. doi: 10.1016/j.chembiol.2011.01.005.

Silva, M.C., Nandi, G.A., Tentarelli, S., Gurrell, I.K., Jamier, T., Lucente, D., Dickerson, B.C., Brown, D.G., Brandon, N.J. and Haggarty, S.J., 2020. Prolonged tau clearance and stress vulnerability rescue by pharmacological activation of autophagy in tauopathy neurons. *Nature Communications*, 11(1), p.3258. doi: 10.1038/s41467-020-16984-1.

Soldatov, N.M., 2012. Molecular determinants of $Ca_v1.2$ calcium channel inactivation. *ISRN Molecular Biology*, 2012, p.691341. doi: 10.5402/2012/691341.

Stan, G.F., Church, T.W., Randall, E., Brown, J.T., Wilkinson, K.A., Hanley, J.G. and Marrion, N.V., 2022. Tau isoform-specific enhancement of L-type calcium current and augmentation

of afterhyperpolarization in rat hippocampal neurons. *Scientific Reports*, 12(1), Article 15231. doi: https://doi.org/10.1038/s41598-022-18648-0.

Sterniczuk, R., Antle, M.C., Laferla, F.M. and Dyck, R.H., 2010. Characterization of the 3xTg-AD mouse model of Alzheimer's disease: part 2. Behavioral and cognitive changes. *Brain Research*, 1348, pp.149-155. doi: 10.1016/j.brainres.2010.06.011.

Storm, J.F., 1987. Action potential repolarization and a fast after-hyperpolarization in rat hippocampal pyramidal cells. *The Journal of Physiology*, 385, pp.733-759. doi: 10.1113/jphysiol.1987.sp016517.

Striessnig, J., Ortner, N.J. and Pinggera, A., 2015. Pharmacology of L-type calcium channels: novel drugs for old targets? *Current Molecular Pharmacology*, 8(2), pp.110-122. doi: 10.2174/1874467208666150507105845.

Striessnig, J., Pinggera, A., Kaur, G., Bock, G. and Tuluc, P., 2014. L-type Ca^{2+} channels in heart and brain. *Wiley Interdisciplinary Reviews: Membrane Transport and Signaling*, 3, pp.15-38. doi: 10.1002/wmts.102.

Tang, J.K.K. and Rabkin, S.W., 2022. Hypocalcemia-Induced QT Interval Prolongation. *Cardiology*, 147(2), pp.191-195. doi: 10.1159/000515985.

Takeda, S., 2019. Tau propagation as a diagnostic and therapeutic target for dementia: potentials and unanswered questions. *Frontiers in Neuroscience*, 13, p.1274. doi: 10.3389/fnins.2019.01274.

Taviaux, S., Williams, M.E., Harpold, M.M., Nargeot, J. and Lory, P., 1997. Assignment of human genes for β2 and β4 subunits of voltage-dependent Ca^{2+} channels to chromosomes 10p12 and 2q22-q23. *Human Genetics*, 100(2), pp.151-154. doi: 10.1007/pl00008704.

Thibault, O., Gant, J.C. and Landfield, P.W., 2007. Expansion of the calcium hypothesis of brain aging and Alzheimer's disease: minding the store. *Aging Cell*, 6, pp.307-317. doi: 10.1111/j.1474-9726.2007.00295.x.

Thibault, O., Porter, N.M., Chen, K.C., Blalock, E.M., Kaminker, P.G., Clodfelter, G.V., Brewer, L.D. and Landfield, P.W., 1998. Calcium dysregulation in neuronal aging and Alzheimer's disease: history and new directions. *Cell Calcium*, 24, pp.417-433. doi: 10.1016/S0143-4160(98)90055-1.

Thomas, G., Chung, M. and Cohen, C.J., 1985. A dihydropyridine (Bay k 8644) that enhances calcium currents in guinea pig and calf myocardial cells. A new type of positive inotropic agent. *Circulation Research*, 56(1), pp.87-96. doi: https://doi.org/10.1161/01.RES.56.1.87.

Tikhonov, D.B. and Zhorov, B.S., 2009. Structural model for dihydropyridine binding to L-type calcium channels. *Journal of Biological Chemistry*, 284(28), pp.19006-19017. doi: 10.1074/jbc.M109.011296.

Tuluc, P., Yarov-Yarovoy, V., Benedetti, B. and Flucher, B.E., 2016. Molecular interactions in the voltage sensor controlling gating properties of Ca_V calcium channels. *Structure*, 24(2), pp.261-271. doi: 10.1016/j.str.2015.11.011.

Vendel, A.C., Rithner, C.D., Lyons, B.A. and Horne, W.A., 2006. Solution structure of the N-terminal A domain of the human voltage-gated Ca2+ channel β4a subunit. *Protein Science*, 15, pp.378-383. doi: 10.1110/ps.051894506.

Wang, Y., Cai, Z., Gosling, M. & Sheppard, D.N., 2018. Potentiation of the cystic fibrosis transmembrane conductance regulator Cl^- channel by ivacaftor is temperature independent. *American Journal of Physiology-Lung Cellular and Molecular Physiology*, 315(5), pp.L846-L857.

Withers, E.G., 2023. Resolution of the interaction site within 4R0N-tau mediating augmentation of L-type calcium current. *Master's Thesis*, University of Bristol.

Wu, J., Yan, Z., Li, Z. et al., 2016. Structure of the voltage-gated calcium channel $Ca_V1.1$ at 3.6 Å resolution. *Nature*, 537, pp.191-196. https://doi.org/10.1038/nature19321

Yasojima, K., McGeer, E.G. & McGeer, P.L., 1999. Tangled areas of Alzheimer brain have upregulated levels of exon 10 containing tau mRNA. *Brain Research*, 831, pp.301-305.

Yin, Y., Gao, D., Wang, Y., Wang, Z.-H., Wang, X., Ye, J., Wu, D., Fang, L., Pi, G., Yang, Y., Wang, X.-C., Lu, C., Ye, K. & Wang, J.-Z., 2016. Tau accumulation induces synaptic impairment and memory deficit by calcineurin-mediated inactivation of nuclear CaMKIV/CREB signaling. *Proceedings of the National Academy of Sciences*, 113(14), pp.E3773-E3781.

Yuan, Y. & Atchison, W.D., 2019. Electrophysiological Neuromethodologies. In: Aschner, M. & Costa, L. (eds) *Cell Culture Techniques*. Neuromethods, vol 145. Humana, New York, NY. https://doi.org/10.1007/978-1-4939-9228-7_11

Xia, X.M., Fakler, B., Rivard, A. et al., 1998. Mechanism of calcium gating in small-conductance calcium-activated potassium channels. *Nature*, 395, pp.503-507. https://doi.org/10.1038/26758

Zhang, S., Zhu, Y., Lu, J., Liu, Z., Lobato, A.G., Zeng, W., Liu, J., Qjang, J., Zeng, S., Zhang, Y., Liu, C., Liu, J., He, Z., Zhai, R.G. & Li, D., 2022a. Specific binding of Hsp27 and phosphorylated Tau mitigates abnormal Tau aggregation-induced pathology. *Elife*, 11, e79898. https://doi.org/10.7554/eLife.79898

Zhang, Y., Wu, K.M., Yang, L. et al., 2022b. Tauopathies: new perspectives and challenges. *Molecular Neurodegeneration*, 17, p.28. https://doi.org/10.1186/s13024-022-00533-z

Zink, C.F., Giegerich, M., Prettyman, G.E. et al., 2020. Nimodipine improves cortical efficiency during working memory in healthy subjects. *Translational Psychiatry*, 10, p.372. https://doi.org/10.1038/s41398-020-01066-z

Commented [DS7]: Which reference is 2022a and which reference is 200b?